

Effect of Metabolic Gases and Water Vapor, Perfluorocarbon Emulsions, and Nitric Oxide on Tissue Bubbles during Decompression Sickness

Thomas Randsøe

This review has been accepted as a thesis together with five original manuscripts by University of Copenhagen 28th of Marts 2014 and defended on 9th of May 2014.

Tutors: Hans Hultborn & Ole Hyldegaard

Official opponents: Niels-Henrik von Holstein-Rathlou, Hanne Berg Ravn & Costantino Balestra.

Correspondence: Laboratory of Hyperbaric Medicine, Department of Anesthesiology, centre of Head and Orthopedics, Rigshospitalet, University Hospital of Copenhagen, Denmark.

E-mail: thomas1623@gmail.com

Dan Med J 2016;63(5):B5237

PREFACE

This study was conducted from February 2009 until May 2012 during my employment at the Faculty of Health Science, Department of Neuroscience and Pharmacology, Panum Institute, University of Copenhagen. The experimental work on which the thesis is based was performed at the Laboratory of Hyperbaric Medicine at the Department of Anaesthesiology, Centre of Head and Orthopaedics, Copenhagen University Hospital Rigshospitalet under the supervision of Ole Hyldegaard, MD, PhD, DMSc. During my employment I attended three international scientific conferences and one PhD Day at the University of Copenhagen with data presentation.

The thesis gives a general overview of the data collection and is based on five experimental studies presented in the following five manuscripts which will be referred to throughout the text by their Roman numerals:

Manuscript I:

Randsøe T, Hyldegaard O. Effect of oxygen breathing and perfluorocarbon emulsion treatment on air bubbles in adipose tissue during decompression sickness. *J Appl Physiol* 2009; 107: 1857–1863

Manuscript II:

Randsøe T, Hyldegaard O. Effect of oxygen breathing on micro oxygen bubbles in nitrogen-depleted rat adipose tissue at sea level and 25 kPa altitude exposures. *J Appl Physiol* 2012; 113: 426–433

Manuscript III:

Randsøe T, Hyldegaard O. Threshold altitude for bubble decay and stabilization in rat adipose tissue at hypobaric exposures. *Aviat Space Environ Med.* 2013 Jul;84(7):675-83

Manuscript IV:

Randsøe T, Hyldegaard O. Treatment of micro air bubbles in rat adipose tissue at 25 kPa altitude exposures with Perfluorocarbon Emulsions and Nitric Oxide. *Eur J Appl Physiol.* 2013 Oct 25.

Manuscript V:

Randsøe T, Meehan, C.F., Broholm, H, Hyldegaard O. Effect of Nitric Oxide on Spinal Evoked Potentials and Survival Rate in Rats with Decompression Sickness. *J Appl Physiol.* 2015; 118(1): 20-28

ABBREVIATIONS

AGE	Arterial gas emboli
CNS	Central nervous system
CO ₂	Carbon dioxide
DCS	Decompression sickness
ECG	Electro cardio gram
EVA	Extravehicular activity
F	Fraction
h	hour
HBO	Hyperbaric O ₂ breathing
i.m.	Intra muscular
MAP	Mean arterial blood pressure
min	Minutes
msw	Meter of seawater
NO	Nitric Oxide
N ₂	Nitrogen
O ₂	Oxygen
P _{alveolar} N ₂	Nitrogen partial pressure in alveolar gas

$P_{\text{arterialN}_2}$	Nitrogen partial pressure in arterial blood
P_{bubbleN_2}	Nitrogen partial pressure in bubble
P_{bubbleO_2}	Oxygen partial pressure in bubble
P_{iO_2}	Partial pressure of inspired oxygen
P_{tissueN_2}	Nitrogen partial pressure in tissue
P_{tissueO_2}	Tissue oxygen partial pressure
scuba	Self-contained underwater breathing apparatus
sec	Seconds
SEP	Spinal evoked potentials
$T_{1/2}$	Halftime
VGE	Venous gas emboli

INTRODUCTION

Decompression sickness - historical background

The clinical syndrome of decompression sickness (DCS) was first reported in 1845 and was initially recognized within the compressed air work environment during mining and tunneling at which increased ambient pressure was used to displace underground water (1). Later workers submerged in compressed caissons were used for sinking bridge piers and excavating bridge foundations during the construction of the Eads Bridge in St. Louis (1871-74) and Brooklyn Bridge in New York (1870-1883). The use of these caissons was responsible for the first major outbreaks of DCS with descriptions of 12 fatalities and 140 workers severely affected (2) and initially coined the words “bends” and “caissons disease” with DCS (3). The history of DCS was in the second half of the nineteenth century mainly related to the compressed air work environment (4-6), but with the invention of the standard diving helmet air-supplied through pipes connected to surface, DCS became associated to underwater activities. The number of divers using diving helmets remained small during the nineteenth century and it was not until J. Cousteau and E. Gagnan introduced the self-contained underwater breathing apparatus (scuba) in 1943, thereby improving maneuverability and minimizing costs, that the way was paved for the widespread recreational diving (7). The open circuit scuba quickly evolved within the military environment and general public and with little experience in underwater activity DCS became frequent within the diving field. This became known as “divers disease” (8).

The advent of balloons and aircrafts capable of attaining significant altitudes in the beginning of the twentieth century brought the clinical syndrome into aerospace medicine known as “altitude DCS” (aDCS). In 1906 the first description of aDCS symptoms was published after a balloon ascent to 8,994 m above sea level (9) and was soon linked to the familiar syndrome known from caissons disease (10). With advancement in technology and the necessity for unpressurized high altitude flight missions during World War II aDCS became a recognized hazard in aviation and before 1959 more than 17,000 cases of aDCS were documented including 17 fatalities (11). Later when man was launched out of earth’s atmosphere in the 1960th, astronauts were exposed to low pressures during extravehicular activities in space (EVA procedures) and exploration of the lunar surface marking a new era of potential aDCS.

Within the last two centuries, DCS has been a recognized hazard from the caisson and the helmet to the development of modern diving systems and introduction of aviation and space travel explaining the wide variety of names linked to the syndrome throughout history.

Nitrogen supersaturation and bubble evolution

The Second Law of Thermodynamics states that the gas content in fluids and tissues during air breathing are in constant equilibrium with the gas content in the respired gas. This equilibrium may enter a state of transient imbalance with alteration in ambient pressure, change in partial pressures and composition of the respired gas (12). Upon steady decompression during a dive or ascent to low pressures at altitude during flight nitrogen gas (N_2), dissolved within tissues and fluids at depth or ground level, must diffuse into the blood and be expired through the lungs, since the quantity of N_2 that can remain dissolved in the organism is directly proportional to the ambient pressure (Henry’s Gas Law) (12). This off-gassing of N_2 dissolved within the different compartments of the body relies on the individual tissue half times of N_2 ($T_{1/2N_2}$) and depends on the tissue perfusion rate, the N_2 solubility in the specific tissue (13, 14) and the N_2 solubility in blood (12, 14). If the decompression phase is too fast, the amount of dissolved N_2 in the various tissues may exceed the physiological means of pulmonary excretion and promote a state of internal/external gas disequilibrium or supersaturation that may generate in situ evolution of N_2 bubbles known as Decompression Sickness (DCS) (12). It thereby follows, that whenever the partial pressures of dissolved gases in the bodily tissues exceed the ambient atmospheric pressure the risk of DCS increases with increasing ratio of N_2 supersaturation ($P_{\text{tissueN}_2}/P_{\text{ambient pressure}}$) as initially described by Haldane (10).

The basic mechanism for DCS is undoubtedly N_2 supersaturation governing the formation of nascent bubbles. However, the underlying mechanism is not truly understood and is associated with a degree of uncertainties. According to the law of Laplace, the surface tension of a bubble is inversely proportional to the bubble radius which opposes bubble development and growth. Consequently, a resulting pressure gradient ($P_{\text{tissueN}_2}/P_{\text{ambient pressure}}$ (10)) of several atmospheres is needed to generate de novo bubble formation in order to overcome the critical bubble radius. This theoretical high pressure gradient far exceeds the much lower critical ratio of tissue supersaturation ($P_{\text{tissueN}_2}/P_{\text{ambient pressure}}$ (10)) necessary to create bubble evolution in vivo (12, 15, 16). The most widely accepted theory encompassing this inconsistency suggest, that DCS bubbles, as a consequence of the Laplace equation, do not evolve de novo, but grow from small preexisting gas entities or micronuclei adhering to the endothelium wall (12, 17, 18).

DCS can develop in the skin or joints giving rise to milder symptoms known as *the bends* or Type I DCS. Large numbers of bubbles may cause more serious symptoms known as Type II DCS, e.g. lung damage, also called *the chokes*, cardiovascular collapse (syncope) or neurological injuries with the white mater of the spinal cord as a commonly affected site leading to sensory dysfunction, paralysis or death (19-21). By means of ultrasound Doppler technology intravascular bubbles can be detected within the cardiovascular system and several reports describe the formation of venous gas embolism (VGE) during DCS (22). However, a clear correlation between VGE load and degree of symptoms has not been established (22) and it therefore seems plausible that symptoms could be associated to bubble formation in tissue. The more so if the lipid content in the tissue is substantial, since the perfusion rate in fatty tissue is low and the N_2 solubility in lipids is high (13, 14). Hence, lipid rich tissues should have a much greater susceptibility of raising the partial pressure of N_2 and thereby an increased risk of generating DCS bubbles. Nevertheless, tissue bubbles are not as easily accessible for experimental

validation as VGE and therefore the role of extravascular bubble formation during DCS is still unresolved.

Despite the potential morbidity when implicating the central nervous system (CNS), the pathophysiological mechanism responsible for spinal cord lesions during DCS is not completely clarified and involves several hypotheses, derived from intravascular as well as extravascular gas bubble formation (23). The intravascular hypotheses includes the “arterial bubble embolism hypothesis” (24) with gas embolism in the spinal cord arterial circulation caused by pulmonary barotraumas or right to left shunts, and the “venous infarction hypothesis” (25) resulting from gas emboli obstructing the epidural vertebral venous plexus due to bubble overload in the pulmonary vessels. The blood-bubble interaction activating the complement system with subsequent coagulation and platelet aggregation may also contribute to the neurological symptoms induced by DCS (26, 27). The extravascular hypothesis involves the liberation of a free gas phase in the lipid rich white matter of CNS as “autochthonous bubbles” causing myelin disruption (28), compressing axons (29) and compromising the local blood supply by exceeding the perfusion pressure (30).

The significance of autochthonous bubbles in tissue is still debated especially with considerations regarding the potential severity of DCS in CNS (23). Although DCS is not a common event, much research has gone into elucidating the pathophysiological mechanisms in order to prevent it, optimize decompression tables and improve treatment modalities.

Metabolic gases and water vapor

Excess N₂ is considered to be the primary gas involved in DCS. If N₂ is the only gas initially present in the newly developed bubble, a gradient for diffusion of other gases present in the surroundings will immediately be established and the gas composition in the bubble will, in accordance to Fick’s first law of gas diffusion, equalize and become identical to the gas content of the surrounding tissue and fluids (31, 32). Due to the metabolic conversion of O₂ into CO₂ in the tissue cells, there is a tension drop or “inherent unsaturation” (33) between the alveolar gas phase and the venous effluent known as the O₂ window (34). The effect of the O₂ window will eventually cause DCS bubbles to shrink regardless of the inert gas they may contain and the magnitude of the O₂ window will increase with increasing P_{Alveolar}O₂/P_{arterial}O₂ during hyperbaric exposures (34, 35). The partial pressures of metabolic gases in tissue, i.e. O₂ and CO₂, and water vapor are believed to be nearly constant and relatively independent from a wide range of inspired PO₂ at hyper- and hypobaric pressures since appropriate levels of PO₂ are a prerequisite for metabolism in living tissue (31, 36, 37). Therefore, upon decompression from a hyperbaric exposure, the tension and fraction of N₂ dissolved in tissues and present in a nascent bubble is relatively large compared to other gases representing only a minor percentage of the total bubble gas composition (31, 36, 37).

During O₂ breathing at hypobaric altitude exposures, the effect of the O₂ window is hampered since levels of P_{Alveolar}O₂/P_{arterial}O₂ decreases with reduction in ambient pressure (34, 35). However, the effect will eventually promote denitrogenation from bubble and tissue and thereby decrease the fraction of N₂ (34, 35). Upon decompression the effect of Boyle’s law is instantaneous and evolved bubbles will expand concomitantly to the decreasing ambient pressure while the partial pressures of all gasses inside the bubble will decrease simultaneously (31, 36, 37). Accordingly the relative constancy of metabolic gases and

water vapor in tissue will generate a partial pressure difference of these gases between bubble and tissue as the bubble enlarge during abrupt reduction in ambient pressure (31, 36, 37); see example in (11). The subsequent inward diffusion will promote bubble growth, an effect supported by the great solubility and permeability (i.e. the product of the diffusion coefficient and solubility coefficient) of metabolic gases and water vapor in lipid tissue (13, 14). Consequently, the resulting fractions of these gases inside the bubble are therefore obliged to increase in inverse proportion to ambient pressure and promote the diffusion of additional inert gas into the bubble (31, 36, 37).

Gas trapped inside body cavities and DCS bubbles is saturated with water vapor that at unaltered temperature remains constant at 47 mmHg (6.27 kPa) disregarding changes in ambient pressure (11). Therefore gas saturated with water vapor will expand with a relatively higher ratio than dry gas during a certain pressure reduction (11). According to the volume pressure relationship of Boyle’s law (V₁P₁ = V₂P₂), a bubble of dry gas performed at sea level pressure and decompressed to 25 kPa will increase with a factor;

$$V_{\text{sea level}} \times 101.3 \text{ kPa} = V_{\text{altitude}} \times 25 \text{ kPa} \Leftrightarrow V_{\text{altitude}} / V_{\text{sea level}} = 101.3 \text{ kPa} / 25 \text{ kPa} = 4$$

When the bubble gas content is saturated with water vapor, the law of Boyle is modified (V₁(P₁ - P_{H₂O}) = V₂(P₂ - P_{H₂O})) (11) and the expansion ratio increases to a factor;

$$V_{\text{sea level}} \times (101.3 \text{ kPa} - 6.27 \text{ kPa}) = V_{\text{altitude}} \times (25 \text{ kPa} - 6.27 \text{ kPa}) \Leftrightarrow V_{\text{altitude}} / V_{\text{sea level}} = (101.3 \text{ kPa} - 6.27 \text{ kPa}) / (25 \text{ kPa} - 6.27 \text{ kPa}) = 5$$

It so follows, that metabolic gases and water vapor constitute a significant contribution to bubble volume and growth at altitude and that this effect increases when lowering the ambient pressure in the hypobaric range. The same gases pose a negligible effect at higher ambient pressures i.e. at sea level preceding hyperbaric exposures (31, 36, 37). *The deduction described above applies to extravascular bubbles. However, since tissue bubbles are not amenable to direct verification the considerations are based on bubble kinetic calculations conducted by Van Liew-, Foster- and Burkard et al. (31, 36, 37). In vivo observations validating these models have to our knowledge not been reported before and therefore investigation demonstrating the contribution of metabolic gases and water vapor in the bubble content during hypobaric exposures seems especially warranted.*

In a previous report by Hyldegaard et al. (38), micro air bubbles (initially containing 79% N₂) were injected into exposed adipose tissue of anaesthetized rats decompressed from sea level and held at 71 kPa (~2,900 m above sea level). O₂ breathing at 71 kPa caused increased growth of air bubbles compared with O₂ breathing at normobaric conditions, but most bubbles at 71 kPa disappeared within the observation period (38). In a recent report (39), micro air bubbles were injected into adipose tissue of rats decompressed from sea level and studied at 25 kPa (~10,376 m above sea level) during O₂ breathing (F_IO₂ = 1) under exact same experimental conditions as in (38). At 25 kPa, air bubbles were found to grow and stabilize without disappearing (39). Further, by means of preoxygenation, injected micro air bubbles were studied in N₂ depleted rat adipose tissue at 25 kPa during O₂ breathing (F_IO₂=1) (39). We found that O₂-prebreathing enhance air bubble disappearance and significantly reduce air bub-

ble growth when compared to non-preoxygenated rats, but preoxygenation did not prevent the growth of air bubbles at 25 kPa despite complete lack of N₂ in tissue (39). The observed variation in bubble growth, disappearance and stabilization at different pressure exposures supports the bubble kinetic models (31, 36, 37) and it was concluded, that metabolic gases and water vapor contribute to bubble volume and growth at an increasing rate when lowering the ambient pressure.

Perfluorocarbon emulsions

Perfluorochemicals are synthetic straight chain or cyclic hydrophobic hydrocarbons originally developed for industry, but later made hydrophilic through an emulsification process and adapted for biological use. PFC has a high capacity for dissolving respiratory gases (40-42) which was demonstrated in 1966 when Clark and Gollan found that a mouse could survive submerged in O₂-enriched liquid PFC (43). However, the most important property of relevance to biology later proved to be as intravascular gas transporters rather than liquid breathing (40-42, 44). The ability of dissolving N₂ has made PFC an obvious candidate for treating DCS and several reports describe a beneficial effect of treating experimental animals with DCS from a hyperbaric exposure. This include reduction in mortality of rodents treated with PFC infusion combined with O₂ or air breathing at sea level upon rapid decompression from a hyperbaric air dive (45-47) as well as improvement in survival rate and morbidity in swine saturation models during combined PFC and O₂ breathing (48, 49).

The advantage of using a PFC as artificial gas transporter may not necessarily include a situation where tissue supersaturation of inert gases co-exists with bubble formation. E.g. PFC administration has also shown enhanced N₂ desaturation and hemodynamic preservation after VGE injury in a rabbit model (50) and absorption of arterial gas embolism (AGE) in rats (51) along with several other reports describing therapeutic properties of PFC on iatrogenic VGE and AGE (52-59) as discussed in a review by Spiess (41). Furthermore, the gas reabsorption and transportation properties of PFC has also been demonstrated by Novotny et al. (60), who found that PFC infusion were able to increase tissue off-gassing of xenon from muscle by some 33% in a dog model and studies performed by Eckmann et Armstead (61), and Herren et al. (58) have shown reduced embolism adhesion to endothelial cells subjected to glycocalyx degradation (61), and preservation of endothelial cells (58) presumably caused by the PFC micelle surfactant surface- and gas transportation properties.

The therapeutic properties of PFC as treatment for DCS relies on the ability to rapidly dissolve and transport N₂ from tissues to the lungs thereby improve the pulmonary excretion and prevent harmful N₂ gas embolisms (41). N₂ has a low solubility in whole blood and in plasma the solubility is 0.015 volume % at 37°C, which stands in contrast to the carrying capacity of PFC emulsions for N₂ that may approach up to 50-volume % at 37°C during normobaric conditions (13, 14, 40, 45). Furthermore, during DCS, PFC emulsions may improve O₂ delivery to ischemic tissues since PFC have an average particle size of less than 0.2 µm in diameter which is considerable smaller than the diameter of red blood cells of 7 µm (62-64). This gives the PFC emulsions a large surface area for gas transfer and presumably an ability to pass through plasma gaps and thereby improve O₂ delivery in hypoxic tissues peripheral to vascular obstructions (63-65). Whereas whole blood with a hematocrit of 41% carries 21% O₂, PFC emulsions may carry up to 60-volume % at 37°C during normobaric conditions (14, 41, 65). Hemoglobin binds O₂ actively in a sigmoid dissociation curve,

while PFC emulsions transport the respiratory gases passively and both O₂ and N₂ dissolve into and come out of solution linearly in accordance to the gas partial pressure gradients between blood and tissue (40-42, 65). This should make PFC emulsions ideal for reducing the risk of DCS by eliminating N₂ and improve oxygenation (40-42, 45). *Despite the obvious advantages of using PFC's as treatment for DCS as demonstrated on survival rate in animal experiments as well as on absorption of VGE and AGE and in spite the uncertainties regarding the potential role of autochthonous bubble formation in tissues, no previous published studies have been conducted describing the influence of PFC on extravascular bubbles in vivo.*

Nitric oxide

Nitric Oxide (NO) releasing agents have on experimental basis in different mammalian species shown to significantly reduce intravascular bubble formation and increase survival rate during DCS from diving. These reports include a short acting NO donor, glycerol trinitrate [nitroglycerine (GTN)], decreasing the intravascular gas formation in pigs decompressed from a saturation dive (66) and humans decompressed from both open-water and hyperbaric air dive (67) as well as a long acting NO donor, isosorbide-5-mononitrate (ISMN), increasing survival rate and reducing intravascular bubble formation in rats (68). The beneficial effect of natural NO has been opposed by administration of a nonselective inhibitor of NO synthase (NOS), increasing intravascular bubble formation and turning a dive from safe to unsafe (69, 70). Though the exact mechanism remains to be established, it has been suggested that NO induces alterations in the hydrophobicity of the endothelial wall, which reduces the stability and density of the nuclei precursors adhering to the surface (66-69) causing less gas to evolve as bubbles. Furthermore, it has also been suggested that NO through augmented blood flow rate may increase the N₂ washout and thereby promote bubble shrinkage (66). However, as discussed by Moon (71) and Wisløff et al. (69), GTN has a very short half time and since reduced flow during decompression appears of minor importance the first hypothesis seems more attractive (69, 71). *Whether NO donors equally promote protection against extravascular tissue bubbles or DCS in CNS as demonstrated on intravascular bubble formation remains to be established.*

The experimental model

The present thesis is based on two experimental models. In the first model, developed by Hyldegaard et al. (38, 39, 72-77), micro gas bubbles were injected superficially into exposed adipose tissue of anaesthetized rats during continuous in vivo observations of bubble size. Changes in bubble growth, shrinkage or stability serve as a visible parameter for gas gradients between injected bubbles, tissue and blood subsequent to alterations in ambient pressure, breathing gas composition, tissue supersaturation, intravascular gas transportation by PFC and changes in blood flow rate by NO donors. In the second model by Hyldegaard et al. (78), a technique measuring spinal cord conductivity by means of peroneal nerve stimulation during the iso-electric phase of the ECG cycle with subsequent measurement of spinal evoked potentials (SEPs) was developed and evaluated on anaesthetized rats. Through measurements of SEPs on rats with DCS, changes in SEPs during different treatment modalities with NO donors serve as an estimate for neurologic deficits evolving from DCS. The use of SEPs as a way of evaluating neurologic DCS is a well known model within the research of DCS.

AIMS

According to the background presented above, the aims of this thesis are:

1. to study the contribution of metabolic gases, O₂ in particular, and water vapor to the bubble content in rat adipose tissue during high altitude exposures.
2. to study the effect of PFC on tissue air bubbles in rats; 1) decompressed to sea level from a hyperbaric air dive, and 2) decompressed from sea level to a hypobaric altitude exposure.
3. to study the effect of NO donors on rats; 1) decompressed to sea level from a hyperbaric air dive through measurements of SEPs and survival rate, and 2) decompressed from sea level to a hypobaric altitude exposure through monitoring of air bubbles in adipose tissue.

HYPOTHESES

Manuscript I

Decompression-induced N₂ bubbles in adipose tissue (79) or micro air bubbles injected into the white mater of the spinal cord (77) have shown to initially grow, then shrink and disappear during O₂ breathing at sea level. This undesirable initial bubble growth has been explained by a greater flux of O₂ into the bubble than the concomitant net flux of N₂ out of the bubble, mostly due to the higher carrying capacity of O₂ than N₂ in blood (14). Accordingly, we hypothesize, that combined O₂ breathing and PFC infusion could promote growth of air bubbles in rat adipose tissue upon decompression to sea level due to the increased O₂ supply by PFC. However, due to PFC's high capacity for dissolving and transporting N₂ in blood, it also seems plausible that the initial bubble growth seen during O₂ breathing could be either reduced or eliminated due to a PFC induced N₂ desaturation.

Manuscript II

If the fraction of O₂, CO₂ and water vapor increases inversely proportional to ambient pressure and contributes to bubble growth during hypobaric exposures at altitude as deduced in (31, 36, 37), we hypothesize, that O₂ bubbles (F_{O₂} = 1; F_{N₂} = 0) in rat adipose tissue depleted from N₂ through 3-h O₂ pre-breathing may grow during O₂ breathing (F_{O₂} = 1) at 25 kPa (~10,376 m above sea level) despite complete lack of N₂ in both tissue and bubble.

Manuscript III

In previous reports (38, 39), micro air bubbles were injected into adipose tissue of rats decompressed from sea level and studied at 71 and 25 kPa (~2,900 and ~10,376 m above sea level) during continued O₂ breathing (F_{O₂} = 1). We found enhanced bubble growth and prolonged disappearance time at 71 kPa when compared to air bubbles at 101.3 kPa (38). At 25 kPa bubbles grew even further and stabilize without disappearing (39). This difference in bubble decay and stabilization at 101.3, 71 and 25 kPa has been ascribed to an increased contribution of O₂, CO₂ and water vapor to the bubble content when lowering the ambient pressure and is consistent with bubble kinetic models (31, 36, 37). Accordingly, we hypothesize, that an ambient pressure

threshold for air bubble decay and stabilization in rat adipose tissue will appear between 71 and 25 kPa.

Manuscript IV

We hypothesize, that air bubble growth and decay in rat adipose tissue during combined O₂ breathing (F_{O₂} = 1) and intravascular PFC and/or NO donor administration at 25 kPa, (~10,376 m above sea level) will be influenced by one or several contradicting mechanisms. Firstly, the greater carrying capacity in blood by PFC could increase the outward diffusion of N₂ from bubble causing faster bubble shrinkage (41). Secondly, increased blood perfusion rate and vasodilation, elicited by an NO donor (isosorbid-5-mononitrate) (80, 81) could improve the gas exchange between bubble and venous blood causing a faster bubble resolution. Opposed to this effect, the fraction of metabolic gases and water vapour will increasingly dominate the bubble content and tissue as ambient pressure decrease (31, 36, 37) and in keeping with the enhanced O₂ transport capacity of blood by PFC (41) and greater blood perfusion rate by NO (82-84), it seems plausible that bubbles may grow even further at altitude due to the increased O₂ supply.

Manuscript V

We hypothesize, that in case NO donors reduce the intravascular bubble formation through elimination of micro nuclei precursors then NO donors may show a protective effect on spinal cord conductivity if the arterial emboli (24), venous infarction (25) or complement activation (26, 27) are the main mechanisms responsible for DCS in CNS. However, if autochthonous bubbles (28-30) are the primary cause for DCS in CNS, removal of intravascular nuclei precursors may sustain survival, whereas the neurological injuries may persist. On the other hand, if NO increases the N₂ washout through augmented blood flow rate, time of administration may be decisive for survival and neurological detriment, due to the short interval of hemodynamic changes caused by nitrates (85).

METHODS

Ethical considerations

The experimental use of anaesthetized rats was approved by a Government-granted license from the Danish Animal Ethical Committee (2012/15/2934-00506) at the ministry of Justice and was conducted in agreement with the Declaration of Helsinki II. All experiments were performed on anaesthetized rats that were euthanized by exsanguinations or by the DCS impact while still in narcosis.

General (manuscript I-V)

Throughout manuscript I to V female wistar rats weighing 250-350 g with free access to food and water were chosen because of their abundant and transparent abdominal adipose tissue into which bubbles can be injected and clearly viewed through a microscope; see Picture 1.

The rats were in all experiments anaesthetized with sodium thiomebumal (100 mg/Kg) intraperitoneally and analgesia buprenorphine (0.01-0.05 mg/kg) subcutaneously while a minor Control Experiment A in IV was anaesthetized with fentanyl 0.315 mg/ml + fluanizone 10 mg/ml (Hypnorm, Veta-Pharma™, K) and midazolam (5 mg/ml) subcutaneously at a start dose of 0.3

ml/100g and supplemented every 30 min at a dose of 0.5mg/100g. In the bubble models (I-IV) the anaesthetized rat was placed supine and fixed to an operating and heating platform on top of an aqueous insulating layer while the rat in the SEP manuscript (V) was placed in a stereotactic frame. For administration of ISMN and GTN in manuscript V, a catheter was placed in the right vena jugularis externa and in all experiments (I-V) a cannula was inserted in the trachea (polyethylene tubing-ID 1.5 mm) and a catheter was placed in the left carotid artery for blood



Picture 1. Injected micro air bubble in rat adipose tissue (40 x magnifications), covered by gas impermeable Mylar and polyethylene membrane. Calibration performed with the metal rod of 200 μ m in diameter at the lower left corner.

pressure registration and administration of PFC in manuscript I and IV. The artery catheter was kept patent by a continuous infusion of non-heparinized denitrogenated saline by means of a syringe pump (SAGE Instruments model 341) at a rate of 1 ml/h. In order to avoid bubble formation during saline infusion in the hypobaric experiments (II-IV), denitrogenated saline was prepared by means of boiling and subsequent storing in sterile gas-tight syringes with Luer lock (39). In all manuscripts (I-V) mean arterial blood pressure (MAP) was measured throughout all experiments by means of a pressure transducer from Edwards Life sciences™ placed inside the chamber. A thermometer placed in the vagina measured body temperature. The vaginal thermometer was connected to a thermostat pre-set at 37°C to maintain a body temperature of 37°C during decompression procedures giving a chamber temperature at 32-36°C. A continuous real time record of temperature and MAP was obtained on a PC via a Pico-log® data collection software.

Succeeding the observation period at the end of the experiment or at the moment of death by manifest DCS, the rat was removed from the pressure chamber and placed under the operating binoculars. With the rat still attached to the operating and heating platform, the thorax and abdomen were opened for a microscopic scan for intra- or extra vascular gas formation before the rat was euthanized by means of exsanguination.

Bubble injection procedure, bubble monitoring and P_{tissueO_2} (manuscript I-IV)

In manuscripts I to IV the abdomen was opened in the midline and the abdominal adipose tissue was exposed. In the hypobaric experiments (II-IV) the cecum was perforated with a 2.0-mm ID cannula and the cannula left in situ to function as drainage for

expanding bowel gases during decompression. The rat was then transferred to the pressure chamber attached to the operating and heating platform. Ones inside the chamber, a Licox™ O_2 microcatheter and a Licox™ thermo probe were placed inside the adipose tissue in manuscript I-III for continuous measurements of tissue O_2 partial pressure (P_{tissueO_2}) and temperature. For all groups in manuscript I-III, P_{tissueO_2} values were registered every 10-15 min during the observation period.

A glass micropipette mounted on a 5 μ l Hamilton syringe was then guided to the exposed adipose tissue and in manuscript I, III and IV two to six air bubbles, in the volume range of 4-500 nl, were then injected superficially and widely separated (i.e. in order to exclude any direct gas exchange between adjacent bubbles), into the adipose tissue using a UMP2™ ultra precision pump from WPI®. For injection of the O_2 bubbles in manuscript II, a transparent cylinder of 10 x 4 cm was flushed with 100% O_2 1.5 l/min for one min to washout atmospheric air. The O_2 content of the transparent cylinder was verified using a Haux Oxysarch™ O_2 detector. Once the O_2 content of the cylinder was verified, the micropipette was guided into the cylinder through a 1 x 1 cm hole and O_2 was withdrawn into the glass micropipette. Two to six O_2 bubbles, in the volume range of 5-800 nl, were then injected superficially and widely separated into the adipose tissue. The numbers of bubbles injected were limited by the surface area of the exposed adipose tissue, partly by assuring their separation from larger blood vessels and nearby peristaltic movements, which could otherwise distort the microscopic picture during the observation period. Injection time lasted 8-15 minutes and subsequently, a gas impermeable Mylar- and polyethylene membrane was positioned over all of the exposed adipose tissue to prevent evaporation.

Bubbles were observed through the chamber window at x 40 magnifications by means of a Leica™ Wild M10 stereomicroscope with a long focal-length objective. Two flexible fiber optic light guides, attached to a Volpo Intralux 5000 lamp, illuminated the bubble field. A Kappa™ CF 15/2 color video camera was fitted to the microscope, and the field was displayed on a TV screen and recorded on DVD recorder Panasonic™ DMR-DH86 (see Fig. 1 in (73)). The recording was then transferred to a computer in order to grab real-time images using the NIH Image version 1.61 program (86) and the visible surface area of the bubbles was calculated by means of automated planimetry. The computer program was calibrated by comparison with a metal rod of 200 μ m in diameter placed on top of the adipose tissue in the observed field. In experiment I, bubble dimensions were recorded after the decompression phase at sea level (101.3 kPa) at every 2-5 min during an observation period of up to 200 min as the maximal bubble observation time or until bubble disappearance. In manuscript II-IV pre-decompression bubble dimensions were obtained and once at altitude, bubble dimensions were recorded periodically at every 2-5 min for up to 215 min as the maximal bubble observation time or until bubbles disappeared from view from which point the rat was recompressed to sea level.

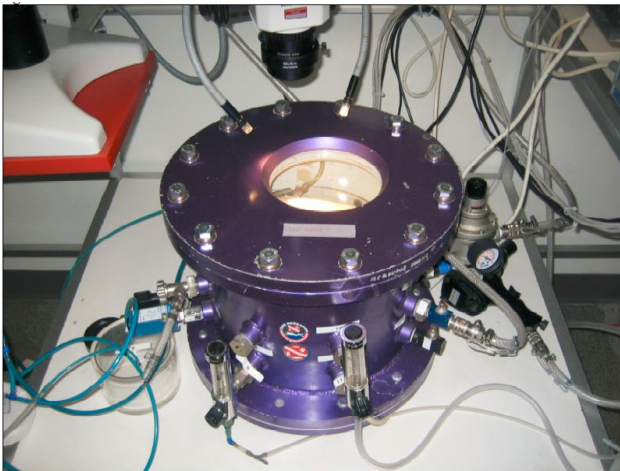
Recording of SEPs (manuscript V)

The cervical vertebral column was exposed through a dorsal midline incision and bore holes were drilled in the 2d and 5th cervical vertebra penetrating the vertebral bone using a dental drill (Bravo Micromotor™, Danish Nordenta A/S, Hard metal round burs RA 1/008+1/009), leaving the dura intact. Two silver electrodes were placed on the dura in the drill holes and fixated with dental cement. Vents were left open to the vertebral canal

by cutting openings in the ligamentum flavum adjacent to the 2d and 5th cervical vertebra to allow the escape of gas accidentally introduced. A polyethylene tube was placed in the operation field as a drain and the incision closed. Both peroneal nerves were dissected free and placed on stimulating electrodes, and the incision closed. The front extremities were perforated with needles and connected to electrodes for Electro Cardio Gram (ECG) registration. SEPs were registered from the cervical electrodes (i.e., over the surface of the dorsal funiculus) during alternate bilateral stimulation of the peroneal nerves and data collected on a PC (CED 1401 with Spike2 software, Cambridge Electronic Design, Cambridge, UK, and NL 800A Linear Constant Current Stimulus Isolator and amplifier from NeuroLog™ Systems by Digitimer Limited). To reduce interference from the ECG, the stimulator was triggered by the R-peak of the ECG with a delay to place the stimulus and SEP in the isoelectric phase of the ECG. During SEP recordings the chamber heating system was briefly disconnected in order to eliminate electrical interference. Stimulation intensity was chosen to give maximal amplitude of the evoked potential and the averaging was done over a 2 min period of consecutive stimulations on each nerve. Before the hyperbaric exposure stimulations were repeated and mean values obtained for the statistical comparison. In the post-decompression observation period at sea level SEPs were recorded at an interval of 10 min in 120 min or until cardiac arrest measured by the ECG.

Pressure chamber, connections and breathing system (manuscript I-V)

Pressurization and decompression was performed in a specially designed pressure chamber with a horizontal viewing port 16 cm in diameter; see Picture 2. The anaesthetized rat was placed supine (I-IV) or in a stereotactic frame (V) on a circular plate that could be removed from the pressure chamber and serve as an operating platform. The platform also contained a built-in heating system which was controlled by a vaginal thermometer maintaining body temperature at an average of 37°C (see Fig. 1 in (73)).



Picture 2. Pressure chamber with a horizontal viewing port 16 cm in diameter, through which bubbles were observed in a microscope and recorded by a video camera.

Once inside the chamber connections were performed for arterial blood pressure registration (MAP), venous catheter, thermometer, Licox, ECG, SEP and stimulation electrodes. In the bottom of the chamber, penetrations were made for a chamber atmosphere heating system consisting of an electrical heater and

a small fan mixing the chamber atmosphere. The rat tracheal cannula was connected to a T-shaped tube in the chamber breathing system and air was supplied continuously at a pressure slightly above chamber pressure. The air provided flowed inside the chamber through an 8-mm ID silicone tube with a small latex rubber breathing bag reflecting the rats' respiratory motion. The T-shaped tube was further connected to an exhaust outlet via a specially designed overboard dump valve. During the pressurization and decompression phase rats breathed air or O₂ spontaneously while connected to the chamber breathing system. In manuscript I-IV all rats continued breathing spontaneously throughout the entire experiments. In manuscript V, ones decompressed to surface, rats were disconnected from the chamber breathing system and the tracheal cannula connected to a rat respirator. Subsequently rats were paralyzed with pancuronium bromide (Pavulon™, 2 mg/kg) by i.m. injection and ventilated artificially by the respirator maintaining a normal arterial CO₂ tension measured with a Radiometer ABL 30 blood gas analyzer. Rats continued air breathing throughout the entire observation period.

Pressurization and decompression profile (manuscript I-V)

Ones the breathing system and connections for the respective chamber penetrations were performed, the top steel lid of the pressure chamber was mounted and for the hyperbaric experiments I and V, the chamber was compressed on air through an inlet fitted with a regulator (AR 425, Baccara) that maintained the desired chamber pressure. For the hypobaric experiments II-IV, a vacuum pump reduced the chamber pressure corresponding to the respective altitudes.

Manuscript I:

Hyperbaric pressurization from 101.3 kPa to 385 kPa absolute pressure (28 msw) in 2 min. Following the 1-h exposure at 385 kPa, rats were decompressed to 101.3 kPa in three stages with two stops (78): 1) decompression from 385 kPa to 304 kPa in 48 sec (101.2 kPa/min) with a stop at 304 kPa for 1 min and 42 sec; 2) decompression from 304 kPa to 202.65 kPa in 1 min (101.3 kPa/min) with a stop at 202.65 kPa for 2 min and 30 sec; 3) decompression from 202.65 kPa to 101.3 kPa (sea level) in 1 min and 30 sec (67.5 kPa/min). Total decompression time was 7 min and 30 sec; see Fig. 1 - Experimental Protocol I.

Manuscript II and IV:

The hypobaric decompression from 101.3 kPa to 25 kPa (~10,376 m above sea level) ambient pressure was performed in three stages with two stops: 1) decompression from 101.3 kPa to 60 kPa in 2 min (~20 kPa/min) with a stop at 60 kPa for 15 min; 2) decompression from 60 kPa to 40 kPa in 2 min (10 kPa/min) with a stop at 40 kPa for 15 min; 3) decompression from 40 kPa to 25 kPa in 2 min (7.5 kPa/min). Total decompression time was 36 min; see Fig. 2 - Experimental Protocol II-IV.

Manuscript III:

The hypobaric decompression from 101.3 kPa to respectively 60, 47 and 36 kPa (~4,205, ~6,036 and ~7,920 m above sea level) ambient pressure was performed over a period of 2-35 min with two stops of 15 min duration at 60 and 40 kPa using the same decompression profile as in experiment II and IV. Total decompression time for the respective groups was: 60 kPa, 2 min; 47 kPa, 18 min and 18 sec with a 15 min stop at 60 kPa; 36 kPa, 34

min and 32 sec with a 15 min stop at 60 and 40 kPa; see Fig. 2 - Experimental Protocol II-IV.

Manuscript V:

Hyperbaric pressurization to 506.6 kPa absolute pressure (40 msw) in 3 min. After 1-h at 506.6, rats were decompressed from 506.6 kPa to 101.3 kPa in three stages with two stops: 1) decompression from 506.6 kPa to 202.6 kPa (10 msw) in 1 min (30 m/min) with a stop at 202.6 kPa for 1 min; 2) decompression from 202.6 kPa to 152 kPa (5 msw) in 17 sec (18 m/min) with a stop at 152 kPa for 43 sec; 3) decompression from 152 kPa to 101.3 kPa in 17 sec (18 m/min). Total decompression time was 3 min and 17 sec; see Fig. 3 - Experimental Protocol V.

Experimental groups

Manuscript I:

Total sample size was 33 rats (N) assigned to 3 experimental groups. All groups were exposed to a 1-h hyperbaric pressurization phase at 385 kPa during air breathing, after which rats were decompressed to sea level (101.3 kPa) and either continued air breathing, switched to O₂ breathing (F_IO₂ = 1.0, 100%) or switched to O₂ breathing (F_IO₂ = 1.0, 100%) combined with Perfluorocarbon emulsion infusion (PFC; Oxygent®, Alliance Pharmaceutical, US) corresponding to 1.16-1.3 ml according to weight; see Fig. 1 - Experimental Protocol I. PFC was administered through the carotid catheter at a dose of 2.7 mg/kg and infused at the moment of reach of surface. Subsequent to decompression, all groups had micro air bubbles injected into the adipose tissue and bubbles (total sample size; n = 77) were studied at normobaric conditions during an observation period for up to 200 min.

Group 1), (N = 13; n = 25); air breathing

Group 2), (N = 9; n = 21); O₂ breathing

Group 3), (N = 11; n = 31); combined O₂ breathing and PFC

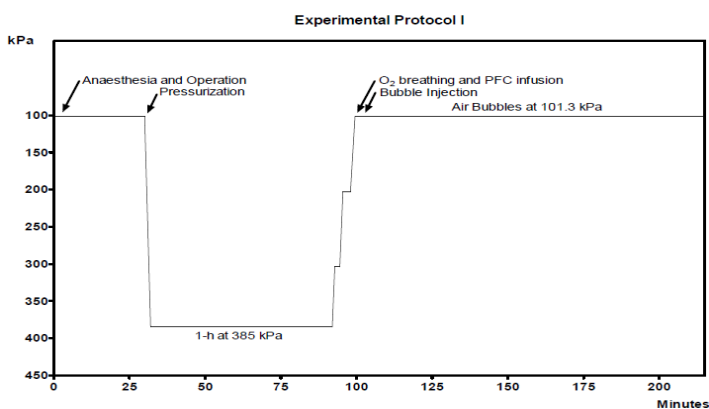


Figure 1 - Experimental protocol I. Following a 1-h period of hyperbaric air dive to 385 kPa, rats were decompressed to sea level in 7,5 min and either continued air breathing, switched to O₂ breathing or switched to O₂ breathing combined with Perfluorocarbon Emulsions infusion. Immediately post decompression rats in all groups had air bubbles injected into exposed adipose tissue and bubbles were studied for 2-h at sea level.

Manuscript II:

Total sample size was 20 rats (N) assigned to 2 experimental groups. Both groups pre-breathed O₂ (F_IO₂ = 1.0, 100%) for a period of 3-h while at sea level (101.3 kPa) in order to assure almost complete N₂ depletion from the adipose tissue. Subsequent, micro O₂ bubbles (total sample size; n = 52) were injected

into the adipose tissue and studied at sea level or exposed to a hypobaric decompression and studied at 25 kPa (~10,376 m above sea level); see Fig. 2 - Experimental Protocol II-IV. At both sea level and altitude, bubble dimensions were recorded periodically for up to 215 minutes or until bubbles disappeared from view at which point the decompressed rat was recompressed to sea level. In both groups, rats continued O₂ breathing throughout the entire experiment. The O₂ bubbles in the decompressed group, were compared to both O₂ bubbles at sea level and to air bubbles of similar size (containing 79% N₂) equally injected into adipose tissue preceded by 3-h of O₂ pre-breathing and studied at 25 kPa under exact similar experimental conditions as described in a previous report (39).

Group 1), (N = 10; n = 27); O₂ breathing at sea level

Group 2), (N = 10; n = 25); O₂ breathing at 25 kPa

Manuscript III:

Total sample size was 15 rats assigned to 3 experimental groups. In all groups micro air bubbles, containing 79% N₂, (total sample size; n = 47) were injected into the adipose tissue at sea level (101.3 kPa) after which rats were switched to O₂ breathing (F_IO₂ = 1.0, 100%) and exposed to a hypobaric decompression from sea level to respectively 60, 47 and 36 kPa ambient pressure (~4,205, ~6,036 and ~7,920 m above sea level); see Fig. 2 - Experimental Protocol II-IV. In all groups, bubble dimensions were recorded periodically for up to 215 minutes or until bubbles disappeared from view from which point the decompressed rat was recompressed to 101.3 kPa.

Group 1), (N = 5; n = 17); O₂ breathing at 60 kPa

Group 2), (N = 5; n = 15); O₂ breathing at 47 kPa

Group 3), (N = 5; n = 15); O₂ breathing at 36 kPa

Manuscript IV:

Total sample size was 30 rats assigned to 3 experimental groups receiving, 1) PFC (Oxygent®, Alliance Pharmaceutical, US), 2) NO donor (isosorbide-5-mononitrate, Dottikon, Switzerland) or 3), combined PFC and NO donor. For the PFC receiving group 1), PFC was administered i.a. through the carotid catheter 2 min prior to decompression at a dose of 2.7 mg/kg corresponding to 1.16-1.3 ml according to weight. For the NO receiving group 2), the anesthetized rats were oroesophageally intubated by means of an atraumatic Hallowell® rodent intubation kit and the rats administered NO intraventricular through the esophageal tube 30-40 min prior to decompression at a dose of 65mg/kg slimed up in 1.16-1.3 ml of saline according to weight. Group 3) was administered both PFC and NO; the volume of saline dissolving NO was 0.5ml and administration of both PFC and NO was as described above under group 1) and 2).

Prior to decompression, all groups had micro air bubbles (total sample size; n = 83) containing 79% N₂ injected into the adipose tissue at sea level (101.3 kPa) after which rats were switched to O₂ breathing (F_IO₂ = 1.0, 100%) and exposed to a hypobaric decompression phase from sea level to 25 kPa (~10,376 m above sea level); see Fig. 2 - Experimental Protocol II-IV. In all groups, bubble dimensions were recorded periodically for up to 215 minutes or until bubbles disappeared from view at which point the decompressed rat was recompressed to 101.3 kPa. The three experimental groups were compared to a control group from a previous report (39), in which rats were decompressed to and held at 25 kPa and injected micro air bubbles of similar size studied under exact same experimental conditions during O₂ breathing alone (F_IO₂ = 1.0, 100%).

Group 1), (N = 10; n = 31); O₂ breathing and PFC
 Group 2), (N = 10; n = 25); O₂ breathing and NO
 Group 3), (N = 10; n = 27); O₂ breathing and combined PFC and NO

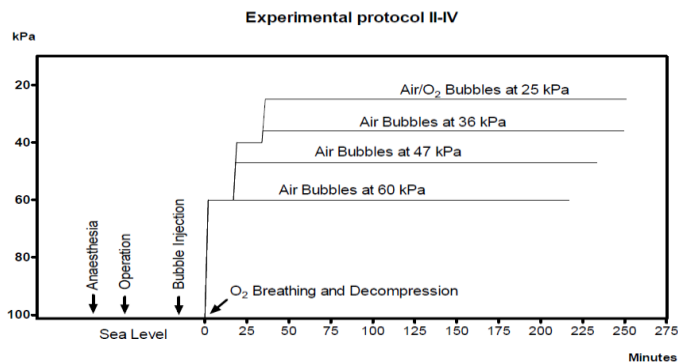


Figure 2 - Experimental protocol II-IV. Experiment II, following a 3-h period of O₂ prebreathing O₂ bubbles were injected into rat adipose tissue and studied at 101.3 (sea level) or 25 kPa. Experiment III, air bubbles were injected into rat adipose tissue and studied at 60, 47 and 36 kPa. Experiment IV, air bubbles were injected into rat adipose tissue and studied at 25 kPa and rats were administered either saline, Perfluorocarbon emulsions, isosorbide-5-mononitrate or Perfluorocarbon emulsion combined with isosorbide-5-mononitrate. Throughout Experiment II-IV, all rats breathed O₂ ones decompressed to altitude.

Manuscript V:

Total sample size was 58 rats (N) and 112 nerves (n) assigned to 6 experimental groups; 1 control group, 2 treatment groups administered ISMN (isosorbide-5-mononitrate, Dottikon, Switzerland) and, 3 treatment groups administered glycerol trinitrate GTN (nitroglycerine, 5 mg/ml in 96% ethanol, Hovedstadens Apotek). All groups were exposed to a 1-h hyperbaric air dive at 506.6 kPa, after which rats were decompressed to sea level (101.3 kPa) and SEP's studied during an observation period for 2-h or until death by DCS; see Fig. 3 - Experimental Protocol V. For the treatment groups, animals were divided into groups receiving ISMN and GTN at sea level before pressurization and at depth before decompression. The control group received 1 ml of saline with an injection rate of 1 ml/min. In the treatment groups, ISMN and GTN was for all animals dissolved in saline giving a total volume of 1 ml and an injection rate of 1 ml/min for group 2), 4) and 6), while the injection rate was 0.2 ml/min (total injection time of 5 min) for group 5), and group 3) was given a bolus injection. The dose of NO donors (except group 3) was chosen according to the hemodynamic effect reported in previous reports (85, 87). In all groups rats breathed air throughout the entire experiment.

Group 1), (N = 12; n = 24); control group; saline i.v. injection initiated 10 min before compression
 Group 2), (N = 12; n = 22); ISMN 300 mg/kg i.v. injection initiated 5-10 min before compression
 Group 3), (N = 8; n = 16); GTN 10 mg/kg i.p. injection 30 min before compression
 Group 4), (N = 10; n = 20); ISMN 300 mg/kg i.v. injection initiated 6 min before decompression
 Group 5), (N = 8; n = 16); GTN 1 mg/kg i.v. injection initiated 8 min before decompression
 Group 6), (N = 8; n = 14); GTN 75 µg/kg i.v. injection initiated 4 min before decompression

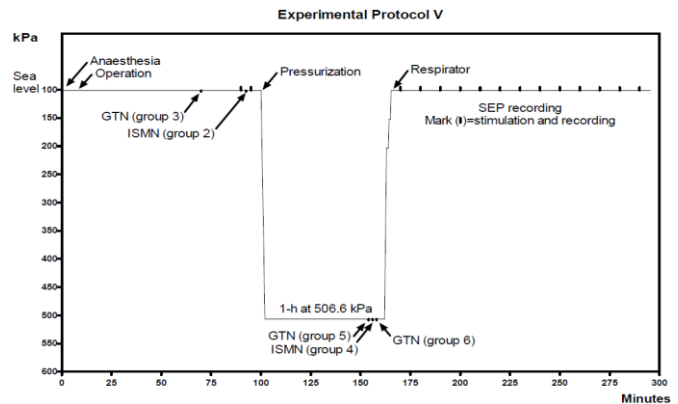


Figure 3 - Experimental protocol V. Anaesthetized rats were exposed to a 1-h hyperbaric air dive to 506.6 kPa and decompressed to 101.3 kPa (sea level) in 3 min and 17 sec during spontaneous air breathing. Following the decompression phase rats were paralyzed and were subsequently mechanically ventilated with air using a respirator. Spinal evoked potentials (SEP's) were measured continuously immediately before the air dive and post decompression during an observation period of 2-h at sea level. Rats were administered either glycerol trinitrate or isosorbide-5-mononitrate at sea level before the dive (group 2 and 3) or during the compression phase (group 4-6).

Evaluation of the anesthesia

Throughout manuscript I-V, the barbiturate thiomebumal intra-peritoneally was used in combination with buprenorphine subcutaneously as the preferable anesthetic drug due to its long acting effects in the female rat (88) providing sufficient time for the surgical and anaesthetic depth during the experimental procedures (89-91). Depth of surgical anaesthesia was maintained by additional top-up of thiomebumal 10 mg/kg until the hind paw withdrawal and tail pinch reflex were absent.

However, it has been suggested that barbiturates may inhibit the NO pathway (92-94), which could cause unwanted effects in the experiments in manuscript IV and V. Accordingly, a control experiment A (N = 10 rats) was conducted in IV, testing the effect of esophageal administered NO on rats anesthetized with fentanyl + fluanizone and midazolam [fentanyl 0.315 mg/ml + fluanizone 10 mg/ml (Hypnorm, Veta-Pharma™, K) and midazolam (5 mg/ml, start dose was 0.3 ml/100g and supplemented every 30 min at a dose of 0.5mg/100g)]. The 10 rats were divided into two groups administered; a) NO donor infusion while anaesthetized; or b) NO donor infusion on non-anaesthetized rats followed by anaesthesia. Both groups underwent same experimental procedures as for group 2-4 in manuscript IV. When comparing group a) (N = 5 rats; n = 14 bubbles) and group b) (N = 5 rats; n = 13 bubbles) with the experimental group 3) in manuscript IV (i.e. NO and thiomebumal + buprenorphine anaesthetized rats) by means of one-way ANOVA testing, there were no differences with respect to bubble growth rate, growth ratio or growth time. The net disappearance rate were found to be significantly faster in group 2) rats compared to control group a) (P = 0.04), but group 2) rats were no different from control group b). There were no differences with respect to the number of bubbles disappearing using Fishers exact.

Further, in manuscript V using thiomebumal anesthetized rats, we found an abrupt decrease in MAP upon administration of GTN and ISMN as previously reported (85, 87) indicating activation of the NO pathway. Based on these results and since NO infusion in thiomebumal anaesthetized rats caused no adverse effects with respect to our primary end point criteria in manuscript IV, we find no need for reservations against anaesthetizing the rats in manuscript IV and V with thiomebumal.

Evaluation of the SEP model (manuscript V):

Experiment A. Stimulations and recordings were done in both directions (i.e. peripheral stimulation with central recording and central stimulation with peripheral recording) to characterize the neuronal path involved. It was found that action potentials traveled in both directions with the same latency, i.e. delay from stimulation to initiation of the first wave. In total the 130 nerves that were stimulated in 68 rats (i.e. 58 rats from experimental group 1-6, 5 rats from *Experiment B* and 5 rats from *Experiment C*, almost all with stimulation of both peroneal nerves) the mean latency before the pressure exposure was 3.36 ms (SD ± 0.22). This is similar to the nerve conduction velocity measured in a previous report and as concluded previously does not allow for a synaptic delay (78).

Experiment B. An extra control group of 5 rats weighing 296.4 g (SD ± 39.1) were monitored without the hyperbaric exposure. Rats were administered 1 ml of saline i.v. and SEP and MAP was recorded for a mean period of 4 h and 37 min (SD ± 11). At the beginning mean MAP was 177.5 mmHg (SD ± 16.6) and remained stable with a slowly shrinking tendency throughout the entire observation period ending up with a mean MAP of 151 mmHg (SD ± 16). The initial mean latency was 3.32 ms (SD ± 0.15) ending up with a mean latency of 3.34 ms (SD ± 0.09) at the end of the observation period. In general there were no changes in the amplitudes of the recorded SEPs.

Experiment C. In order to improve readability of the SEP's by reducing electrical noise from the muscles, rats in the experimental group 1-6 were paralyzed and connected to a respirator. To clarify whether the respirator could influence survival rate or conductivity of the spinal cord during DCS an extra group (*Experiment C*) was monitored and exposed to a 1-h hyperbaric air dive similar to the experimental control group 1). Ones decompressed to sea level, rats in the *Experiment C* continued breathing air spontaneously through the chamber breathing system instead of getting paralyzed and connected to the respirator. In the *Experiment C* (N = 5 rats, n = 9 nerves), mean weight of 321.2 g (SD ± 10), 4 rats died within a period of 2-62 min post decompression while 1 rat survived the observation period. Mean survival time for the whole group was 58 min (SD ± 37.8) with a median range of 60 min (2-120). Before the pressure exposure, MAP was stable with a mean of 171 mmHg (SD ± 19.8) and mean latency for the 9 nerves were 3.56 ms (SD ± 0.18). Following the hyperbaric exposure, conductivity was immediately lost in 3 nerves and the amplitude at the last measurable SEP was reduced in 5 out of 6 nerves. Last measured mean latency was 3.7 ms (SD ± 0.25), mean SEP disappearance time was 45 min (SD ± 47.7) with a median range of 41 min (0-120) and mean MAP at SEP disappearance was 132.2 mmHg (SD ± 38.9). All of the 4 rats dying during the observation period had ample intravascular gas formation, while no intravascular gas was found in the rat surviving.

Comparing experimental control group 1) with the *Experiment C*, there was no significant differences regarding weight, MAP, survival time or spinal cord conductivity. Accordingly, we found no reservations towards using a respirator.

DATA ANALYSIS AND STATISTICS

Statistical analysis was performed using GraphPad, InStat version 3.06 for windows (95) or SPSS (96) and statistical significance was for all comparisons defined as $P < 0.05$.

Bubble growth and decay (manuscript I-IV)

In manuscript I-IV bubble growth (growth time, growth rate, growth ratio) and decay (disappearance time, disappearance rate and disappearance) were evaluated. When several bubbles were studied in one animal, their mean value was used for each animal in the statistical comparison.

Bubbles were analyzed with respect to bubble "growth time" (min) defined as time of observed bubble growth from first observation at sea level (I) or altitude (II-IV) until time of maximal bubble size was measured. Bubbles were also analyzed with respect to mean "growth rate" ($\text{mm}^2 \times \text{min}^{-1}$) from the time of first observation at sea level (I) or altitude (II-IV) until maximal bubble size was measured. If a bubble did not grow but shrank, growth rate was given a negative value indicating shrinkage. Similarly bubbles were measured with respect to bubble "disappearance time" (min) defined as first observation at sea level (I and II) or altitude (II-IV) until bubbles disappeared. If a bubble did not disappear within the observation period, cut of time was set to 200 (I) or 215 (II-IV) min as the last point of observation. Bubble "disappearance rate" was expressed as the mean net disappearance rate ($\text{mm}^2 \times \text{min}^{-1}$), i.e. the slope of a line from the first measured bubbles size during observation at sea level (I-II) or altitude (II-IV) to disappearance of the bubble. If a bubble did not disappear, the mean net disappearance rate was calculated as the slope of the line connecting the first observation at sea level (I) or altitude (II-IV) with the last observation. If a bubble did not shrink but grew, disappearance rate was given a negative value indicating growth.

Mean values of calculated bubble growth time, growth rates, disappearance time and disappearance rates are given \pm SD. To examine whether the differences between two mean values of calculated bubble growth times, disappearance times, growth rates or disappearance rates were different from zero, test for normality by means of Kolmogorov and Smirnov (KS) test followed by either parametric one-way analysis of variance (ANOVA) or nonparametric ANOVA (Kruskal-Wallis Test) was performed on the difference between mean values in the different treatment groups. The difference between mean values in the treatment groups were then analyzed by use of the Bonferroni Multiple Comparisons Test of means between groups or Dunn's test.

Furthermore, bubbles were analyzed with respect to their mean "growth ratio" using a nonparametric analysis of variance ANOVA (Kruskal-Wallis Test). Bubble growth ratio is calculated as maximal measured bubble size in the observation period divided with the first observed bubble size in the observation period at sea level (I) or altitude (II-IV).

Bubbles were also compared with respect to "bubbles disappeared" or "bubbles not disappeared" in the observation period by means of a contingency table using Fishers Exact test. Statistical analysis by means of ANOVA (Kruskal-Wallis test) was performed between groups with respect to possible differences in the size of injected bubbles, time from decompression to first observation at 60, 47, 36, (III) and 25 kPa (II and IV), and observed bubble size caused by the immediate effect of decompression to the respective altitudes (II-IV).

P_{tissueO_2} (manuscript I-III)

The mean values of P_{tissueO_2} (mmHg) measurements at sea level (I-II) or altitude (II-III) were calculated for each animal. To examine whether the difference between two mean values of P_{tissueO_2} measurements were different from zero, test for normality by means of Kolmogorov and Smirnov (K) test followed by one-way

ANOVA was performed on the difference between mean values in the different treatment groups. The difference between mean values of the various treatment groups were then analyzed by use of Bonferroni Multiple Comparisons Test of means between groups or unpaired Mann-Whitney test.

SEPs (manuscript V)

The majority of rats in all groups died or lost the nerve conductivity during the observation period. Accordingly, the mean SEP recorded before the pressure exposure was compared to the last value obtained at the end of the observation period or the last measurable value before loss of conductivity. SEPs were measured as *latency*, defined as delay from stimulation to initiation of the first wave and expressed in ms, and *amplitude* defined as displacement from the baseline and expressed in mv. In each group, the last measurable latency was compared to the mean pre-compression latency and the last measurable amplitude was compared to the mean pre-compression values and graded as *unaffected* (less than 5% reduction) or *reduced* (more than 5% reduction). Further, time from beginning of the observation period until loss of conductivity was for each nerve defined as *SEP disappearance time* and expressed in min. When the conductivity was compromised immediately post-decompression SEP disappearance time was set to zero. When conductivity was maintained during the entire observation period, SEP disappearance time was set to 120 min. Rats were also measured with respect to *survival time*, defined as time from beginning of the observation period until death by cardiac arrest and expressed in min. If a rat survived the observation period, survival time was set to 120 min. Mean MAP before the pressure exposure and mean MAP at the time of SEP disappearance was given in mmHg. If a SEP was preserved throughout the observation period, MAP at SEP disappearance was defined as the last recorded MAP at the end of the observation period. Mean values of weight, MAP, latency, SEP disappearance time and survival time are given \pm SD.

To examine whether the differences between two mean values of weight, MAP, SEP disappearance time and survival time were different from zero, test for normality by means of Kolmogorov and Smirnov (KS) test followed by nonparametric analysis of variance ANOVA (Kruskal-Wallis Test) was performed on the difference between mean values in the different treatment groups. The difference between mean values in the treatment groups were then analyzed with multiple comparisons test of means between groups by use of Dunn's test. Student's *t* test (paired) was performed on each group to see whether the mean change in latency was different from a mean of zero.

Rats were also compared with respect to *death or survival* within the observation period, and the last measured amplitudes in the different treatment groups were compared to the last measured amplitudes in the control group by means of a contingency table using Fishers Exact test.

RESULTS

Manuscript I

Effect of air and O₂ breathing \pm PFC infusion on air bubbles in rat adipose tissue at 101.3 kPa

Treatment group	Growth time Min ⁻¹	Growth rate mm ³ x min ⁻¹	disappearance rate min ⁻¹ x min ⁻¹	Bubbles Disappeared ^{*)}	Bubble growth ratio > 1.034 ^{*)}
Air breathing N = 13 animals n = 25 bubbles	86.0 \pm 26.8 ^{*)}	2.54 \pm 1.46 ^{*)}	-420 \pm 806 ^{*)}	0 of 25	25 of 25 ^{*)}
O ₂ breathing N = 9 animals n = 21 bubbles	46.3 \pm 24.2 ^{*)}	5.5 \pm 3.35 ^{*)}	3.85 \pm 3.57 ^{*)}	17 of 21	20 of 21 ^{*)}
O ₂ breathing + PFC N = 11 animals n = 31 bubbles	31.0 \pm 9.0	8.27 \pm 7.45	7.48 \pm 4.29	29 of 31 ^{*)}	24 of 31

Table 1 *) Values are means \pm SD. *J Appl Physiol* 2009; 107: 1857–1863

ANOVA followed by multiple comparison of means between groups showed that bubble growth time was significantly longer during air breathing compared with both O₂ breathing and combined O₂ breathing with PFC infusion ($P < 0.05$)¹⁾; see Table 1 and Fig. 4a-4c. Bubbles displayed a significantly faster growth rate during combined O₂ breathing with PFC infusion than during air breathing ($P < 0.05$)²⁾. The net disappearance rate of bubbles during O₂ breathing was significantly faster than during air breathing ($P < 0.01$)³⁾ and combined O₂ breathing with PFC infusion caused a significantly faster net disappearance rate than during both air ($P < 0.0001$) and O₂ breathing ($P < 0.05$)⁴⁾. Mean bubble growth ratio was significantly smaller during combined oxygen breathing with PFC infusion compared with air breathing ($P < 0.05$)⁵⁾. Fisher's exact test showed that the number of bubbles that disappeared in the observation period during both oxygen breathing and combined oxygen breathing with PFC infusion was significantly different from air breathing ($P < 0.0001$)⁶⁾. There was a significant difference in mean P_{tissue}O₂ values in air-breathing animals compared with oxygen and combined oxygen breathing and PFC-treated animals ($P < 0.05$). The greater P_{tissue}O₂ during combined PFC infusion and oxygen breathing compared with oxygen breathing alone was not quite significant ($0.1 > P > 0.05$).

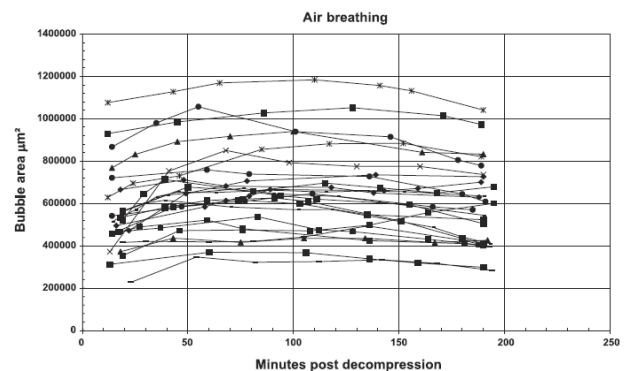


Figure 4a

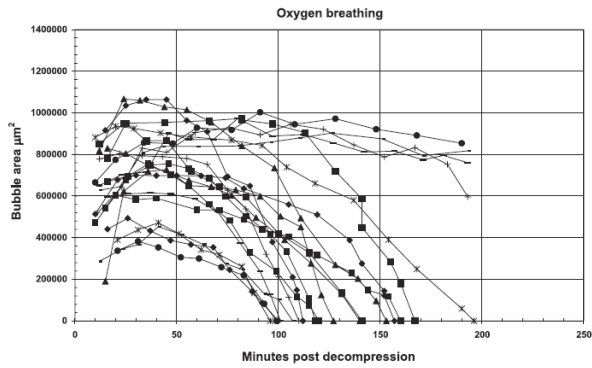


Figure 4b

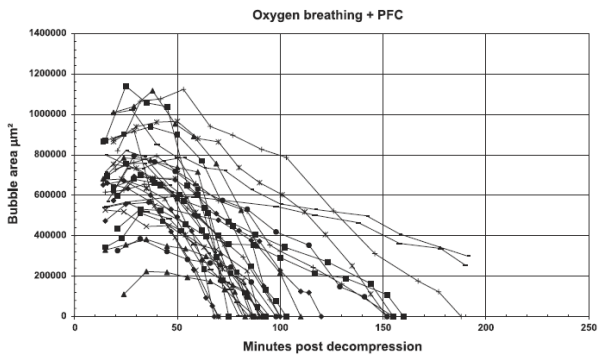


Figure 4c

Figure 4a, 4b and 4c. Effect of air, O₂ and combined O₂ breathing and PFC infusion on air bubbles in rat adipose tissue at sea level preceded by 1-h hyperbaric exposure at 385 kPa during air breathing. Individual symbols represent one bubble curve. *J Appl Physiol* 2009; 107: 1857–1863

Manuscript II

O₂ and air bubble growth rate, disappearance rate, disappearance time and bubble disappearance in N₂ depleted rat adipose tissue during oxygen breathing at 101.3 kPa and 25 kPa

Treatment group	Growth rate (mm ³ × min ⁻¹ × mm ⁻³)	Net disappearance rate (mm ³ × min ⁻¹ × mm ⁻³)	Disappearance time (min. *)	Bubbles disappeared	P _{tissue} O ₂ (mmHg)
O ₂ bubbles at 101.3 kPa N = 10 ³ n = 27 Bubbles	-0.02 ± 0.008 ¹⁾	0.02 ± 0.008 ²⁾	30 ± 7.9 ³⁾	25 of 25	122 ± 29 ⁴⁾
O ₂ bubbles at 25 kPa N = 10 ³ n = 25 Bubbles	0.012 ± 0.014 ²⁾	0.01 ± 0.004 ²⁾	125 ± 52 ²⁾	23 of 27	69 ± 46 ⁴⁾
Air bubbles at 25 kPa ¹⁾ N = 10 ³ n = 20 Bubbles	0.007 ± 0.008	0.0022 ± 0.0068	159 ± 20	8 of 20 ¹⁾	X

Table II *) Values are means ± SD. **) Data from (39). *J Appl Physiol* 2012; 113: 426–433

ANOVA followed by multiple comparisons among the groups showed that the O₂ bubble growth rate at 25 kPa altitude were

faster as compared to O₂ bubbles at 101.3 kPa sea-level pressure (P<0.001)¹⁾ in which no bubble growth were observed (i.e. the negative growth rate; see Table 2 and Fig. 5a and 5b). O₂ bubble net disappearance rate and disappearance time were significantly faster at 101.3 kPa in comparison to O₂ bubbles at 25 kPa altitude (P<0.01 and P<0.001 respectively)^{2,3)}. P_{tissue}O₂ values were significantly higher at 101.3 kPa when compared to 25 kPa (P = 0.0147)⁴⁾.

When injected micro O₂ bubbles are compared to our previously injected micro air bubbles (39) (consisting of 79% N₂) at 25 kPa, bubble growth and net disappearance rates are not different from each other (p>0.05); see Table 2 and Fig. 5c and 5d. Further, air bubble disappearance times were not different from the present O₂ bubbles disappearance times at 25 kPa altitude. However, more O₂ bubbles disappeared within the observation phase as compared to air bubbles (39) by means of Fishers Exact Test (P=0.0019)⁵⁾.

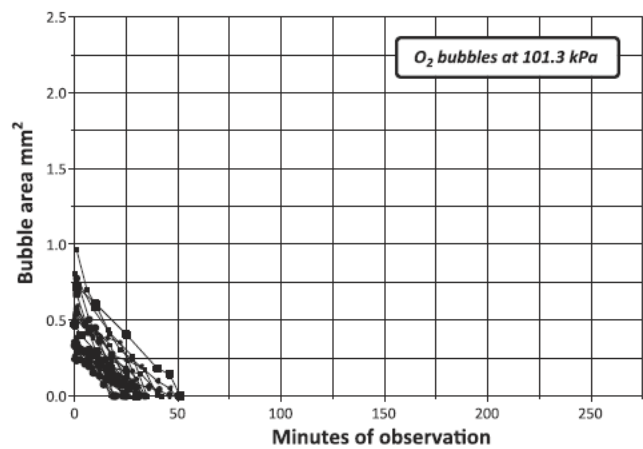


Figure 5a

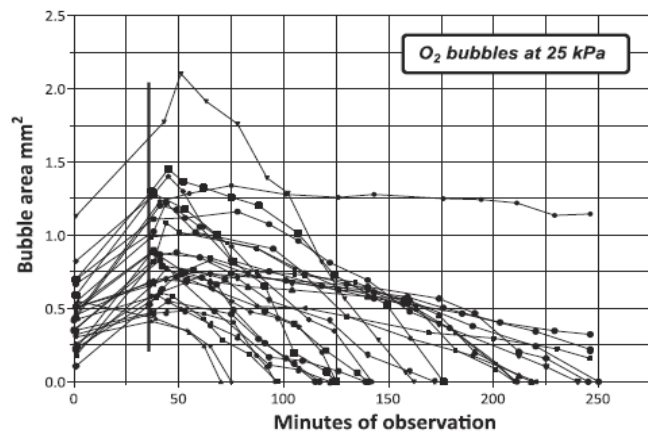


Figure 5b

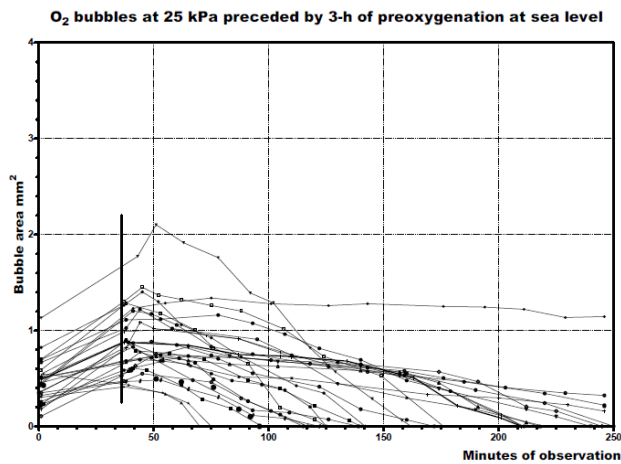


Figure 5c

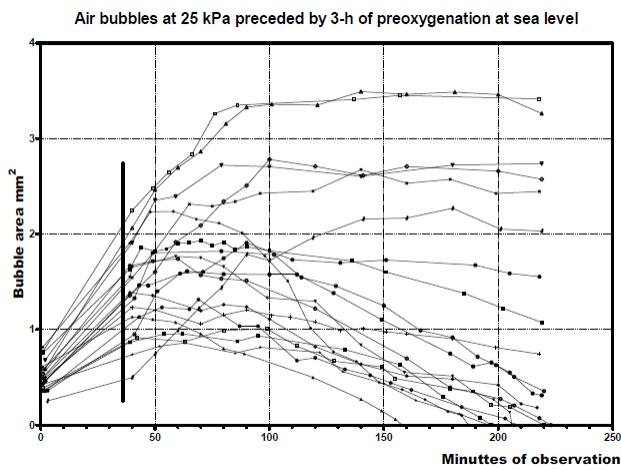


Figure 5d

Figure 5a, 5b, 5c and 5d. Effect of O₂ breathing on O₂ bubbles at sea level and at 25 kPa and effect of O₂ breathing on air bubbles at 25 kPa. In all groups rats pre-breathed O₂ for 3-h to eliminate tissue N₂. Vertical bar indicates barometrical pressure of 25 kPa. Fig. 2a and 2b are identically scaled in order to compare O₂ bubbles at sea level and 25 kPa. Fig 2c and 2d are identically scaled in order to compare air and O₂ bubbles at 25 kPa. Fig. 2b and 2c show the same graph with different scaling. Fig. 1ld, data from (39). Fig. 1la, 1lc and 1lb data from *J Appl Physiol* 2012; 113: 426–433

Manuscript III

Air bubble growth rate, time, ratio, net disappearance rate, P_{tissue O₂} and bubble disappearance/stabilization in rat adipose tissue at 60, 47 or 36 kPa altitude exposures during O₂ breathing

Treatment group	Growth rate mm ² × 10 ³ × min ⁻¹ *)	Growth time min. *)	Growth ratio *)	Net disappearance rate mm ² × 10 ³ × min ⁻¹ *)	P _{tissue O₂} mmHg *)	Bubbles disappeared **) Bubbles stabilized ***)
Air bubbles at 60 kPa n = 5 Animals N = 17 Bubbles	4.3 × 10 ⁻³ ± 3.2 × 10 ⁻³	44 ± 14	1.51 ± 0.46	2.0 × 10 ⁻³ ± 0.9 × 10 ⁻³	180 ± 9 ⁽¹⁾	14 of 17**) 3 of 17 ***)
Air bubbles at 47 kPa n = 5 Animals N = 15 Bubbles	3.4 × 10 ⁻³ ± 4.7 × 10 ⁻³	23 ± 24	0.89 ± 0.5	4.4 × 10 ⁻³ ± 0.7 × 10 ⁻³ (1)	146 ± 20 ⁽¹⁾	14 of 15**) 1 of 15 ***)
Air bubbles at 36 kPa n = 5 Animals N = 15 Bubbles	5.6 × 10 ⁻³ ± 2.4 × 10 ⁻³	32 ± 19	1.03 ± 0.34	3.7 × 10 ⁻³ ± 1.5 × 10 ⁻³	99 ± 14	3 of 15 ⁽¹⁾ **) 12 of 15 ***)

Table 3 *) Values are means ± SD. **) Bubbles disappearing ***) Bubbles stabilizing. *Aviat Space Environ Med.* 2013 Jul;84(7):675-83

Net disappearance rate was significantly faster at 47 kPa when compared to 60 kPa ($P < 0.05$)¹⁾, while the observed difference when comparing 60 with 36 kPa altitude levels did not quite reach statistical difference ($0.1 > P > 0.05$); see Table 3 and Fig. 6a-6c. Fishers exact test showed that the number of bubbles disappearing in the observation period at 36 kPa was significantly different from both 60 ($P < 0.001$) and 47 kPa ($P < 0.0001$)²⁾. There were no differences when comparing 60 with 47 kPa. ANOVA showed that mean P_{tissue O₂} values were different ($F(2,17) = 46.23, P < 0.0001$); see Table 3 and Fig. 7. Bonferroni post-hoc analysis showed that mean P_{tissue O₂} values were significantly higher at 60 kPa than at both 47 ($P < 0.01$) and 36 kPa ($P < 0.001$)³⁾, while values were significantly higher at 47 kPa than at 36 kPa ($P < 0.001$)⁴⁾.

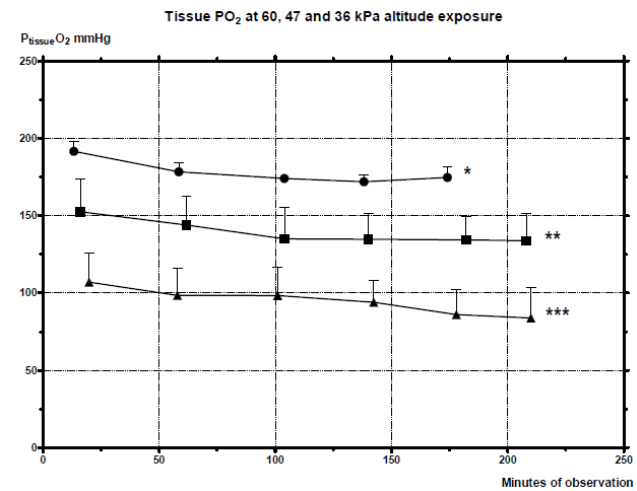


Figure 7. Effect of O₂ breathing (F_IO₂ = 1) and decompression on adipose tissue O₂ partial pressure (P_{tissue O₂}). Each curve represents mean P_{tissue O₂} ± SD (mmHg) during the observation period at altitude. * P_{tissue O₂} at 60 kPa altitude exposure. ** P_{tissue O₂} at 47 kPa altitude exposure. *** P_{tissue O₂} at 36 kPa altitude exposure. *Aviat Space Environ Med.* 2013 Jul;84(7):675-83

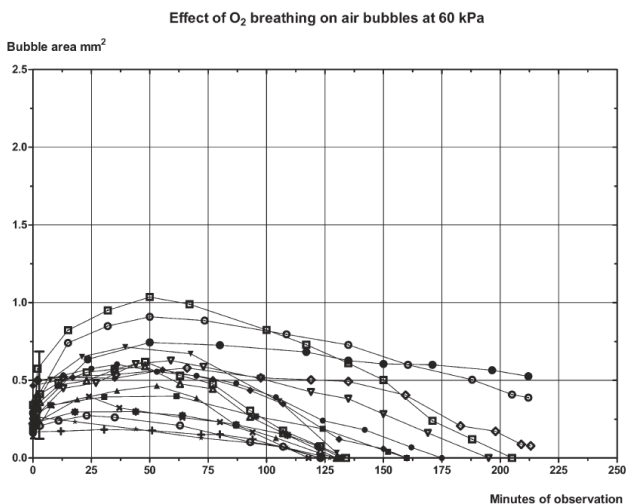


Figure 6a

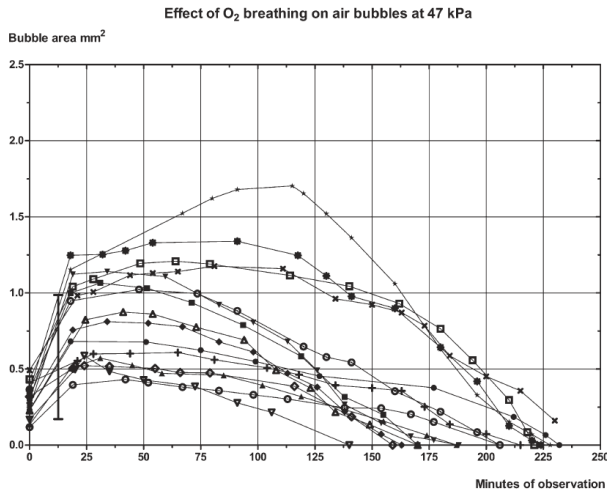


Figure 6b

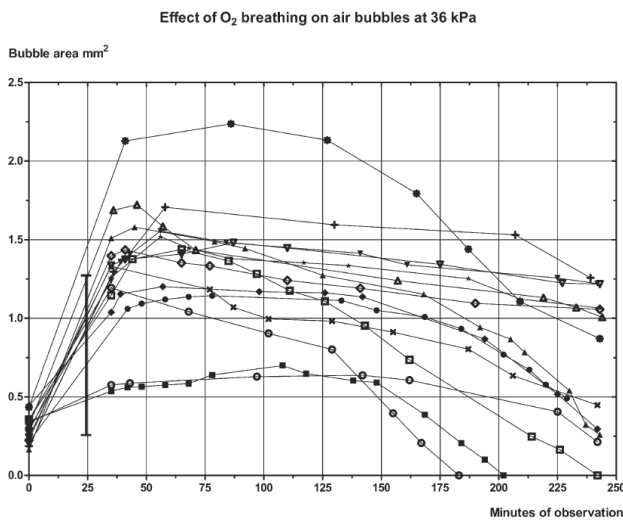


Figure 6c

Figure 6a, 6b and 6c. Effect of O₂ breathing and decompression from sea level to 60, 47 and 36 kPa on air bubbles in adipose tissue. Each curve represents one bubble. Vertical bar indicates time of arrival at respective altitudes. *Aviat Space Environ Med.* 2013 Jul;84(7):675-83

Manuscript IV

Effect of PFC, NO and combined PFC and NO on air bubble growth and decay in rat adipose tissue at 25 kPa altitude exposures during O₂ breathing

Treatment group	Growth rate mm ² x min ⁻¹ *	Growth time min. *	Growth ratio *	Net disappearance rate mm ² x min ⁻¹ *	Bubbles disappeared *** stabilized ****
PFC N = 10 Animals n = 31 Bubbles	0.025 ± 0.024	64.7 ± 28.1 ¹	1.63 ± 0.37	0.0001 ± 0.005	2 of 31*** 29 of 31****
NO N = 10 Animals n = 25 Bubbles	0.013 ± 0.008	63.8 ± 23.3 ¹	1.49 ± 0.40	0.0011 ± 0.0043	1 of 25*** 24 of 25****
PFC and NO N = 10 Animals n = 27 Bubbles	0.02 ± 0.009	77.8 ± 53.4	1.62 ± 0.43	0.0012 ± 0.0073	3 of 27*** 24 of 27****
Control group** N = 8 Animals N = 18 Bubbles	0.012 ± 0.007	121 ± 53.4	1.79 ± 0.33	-0.0045 ± 0.0041	0 of 18*** 18 of 18****

Table 4 *) Values are means ± SD. **) Control group breathing O₂ alone; data from (39). ***) Bubbles disappearing. ****) Bubbles stabilizing. *Eur J Appl Physiol.* 2013 Oct 25.

When the experimental groups (2-4) are compared to the control group breathing O₂ alone from our previous report (39), ANOVA

followed by multiple comparisons showed that bubble growth time was significantly longer during O₂ breathing alone (39) when compared to rats receiving PFC or NO ($P < 0.042$ and $P < 0.037$)¹ respectively; see Table 4 and Fig. 8a-8c. No other significant differences between the experimental groups (2-4) and the control group breathing O₂ alone (39) were found concerning growth rate, or ratio, nor with respect to net disappearance rate. When the number of bubbles disappeared within the observation period are examined, Fishers Exact Test showed no significant difference ($P > 0.05$) in bubble disappearance within the present experimental groups (2-4) or when compared to the control group breathing only O₂ (39).

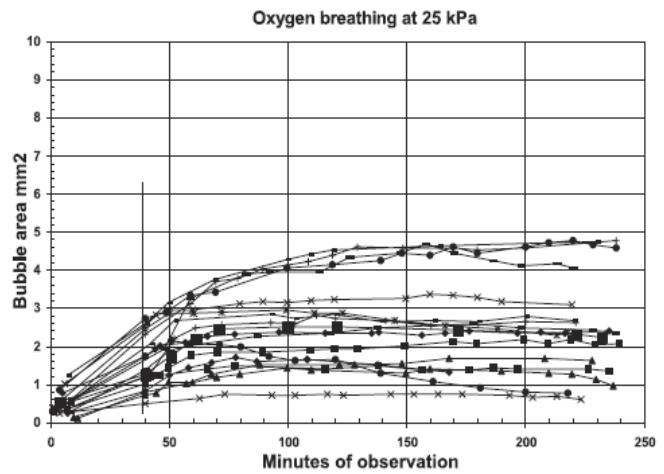


Figure 8a

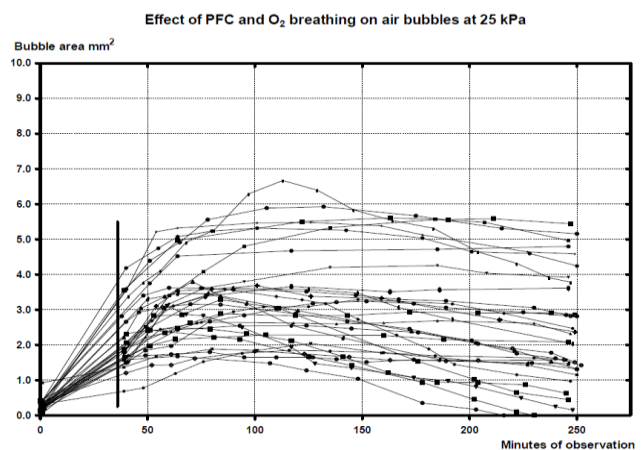


Figure 8b

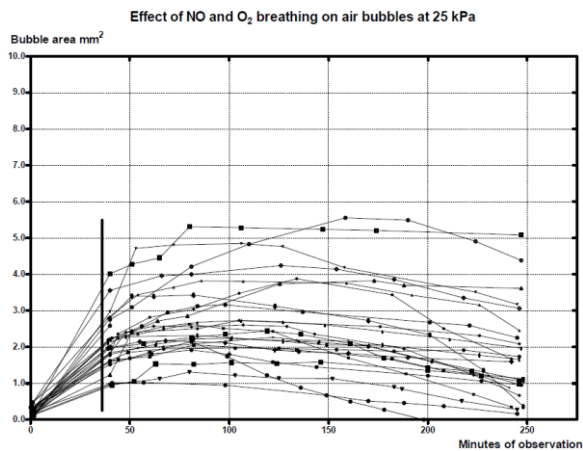


Figure 8c

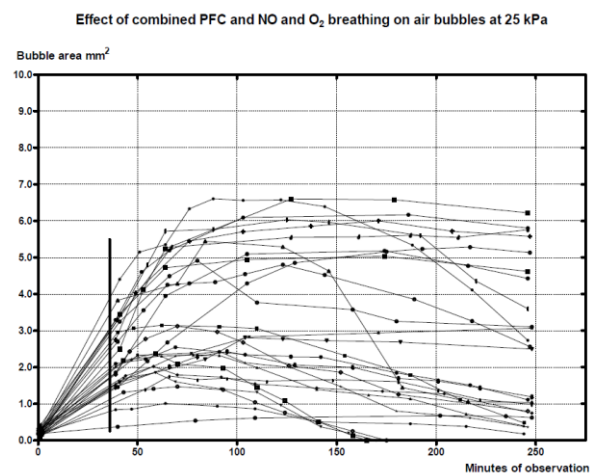


Figure 8d

Fig. 8a, 8b, 8c and 8d. Effect of O₂ breathing and decompression to 25 kPa on air bubbles in adipose tissue during O₂ breathing alone (data from (39)), PFC infusion, NO infusion, and during combined PFC and NO infusion. Each curve represents one bubble. Vertical bar indicates time of arrival at 25 kPa. *Eur J Appl Physiol.* 2013 Oct 25.

Manuscript V

Effect of ISMN and GTN administration before and during a hyperbaric exposure on spinal cord conductivity and survival in rats with DCS

Treatment group	Group 1 Saline	Group 2 ISMN 300 mg/kg iv. 5-10 min before compression	Group 3 GTN 10 mg/kg ip. 30 min before compression	Group 4 ISMN 300 mg/kg iv 6 min before decompression	Group 5 GTN 1 mg/kg iv. 8-3 min before decompression	Group 6 GTN 75 µg/kg iv. 4 min before decompression
N = rats	12	12	8	10	8	8
n = nerves	24	22	16	20	16	14
Weight (g ^{*)})	305.6 ± 19	307.2 ± 17.2	301.1 ± 19.2	305.8 ± 17.5	304.2 ± 20	306 ± 24.5
Survival	2 of 12	2 of 12	0 of 8	3 of 10	0 of 8	2 of 8
SEP disappearance min Mean *) Median range	43.7 ± 39.9 26 (0-120)	42.3 min ± 35.2 33 (0-120)	18.9 ± 13.6 ¹ 12.5 (0-53)	42.1 ± 41.2 23 (0-120)	13.7 ± 12.5 ² 12 (0-43)	32.6 ± 39.2 12 (0-120)
Survival time min Mean *) Median range	55.7 ± 35.4 44 (17-120)	62 min ± 32 50 (23-120)	40.5 ± 27.2 27 (17-93)	65.3 ± 44.9 49 (20-120)	27.9 ± 19.1 ³ 19 (9-67)	51 min ± 43.3 31 (20-120)

Table 5 *) Values are means ± SD.

ANOVA followed by multiple comparisons among the groups showed that SEPs disappeared significantly faster in group 5) when compared to both group 1) ($P < 0.05$) and group 2) ($P < 0.01$)², while SEPs in group 3) disappeared significantly faster than group 2) ($P < 0.05$)¹; see Table 5 and Fig. 9a-9e for SEP example. There was no difference in SEP disappearance times between the remaining groups. The survival time was significantly shorter in group 5) than group 2)³, while there was no difference in survival time among the rest of the groups.

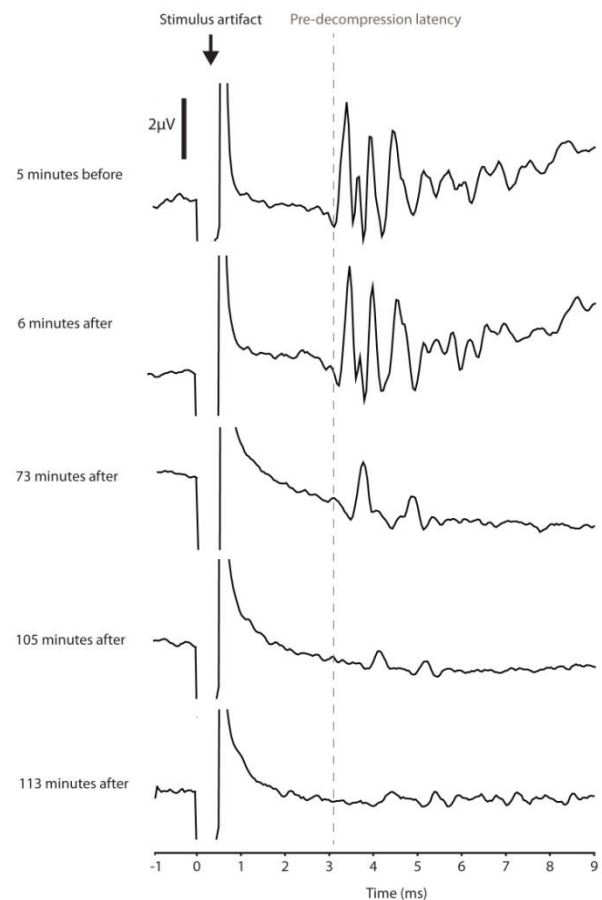


Figure 9.(97) Illustrated are spinal evoked potentials for one rat from group 2, with ISMN administered at sea level prior to the hyperbaric exposure. Spinal evoked potentials are demonstrated before, and at various time intervals (as indicated) after the dive. Stimulus artifacts have been truncated.

DISCUSSION

Validity of the bubble model (manuscript I-IV)

The model used in the present experiments is based on injected gas in tissue and it is therefore reasonable to question whether injected bubbles in abdominal adipose tissue are comparable to those evolved from DCS. It could be argued, that use of decompression induced DCS bubbles rather than injected bubbles, would constitute more genuine conditions, encompassing the broad complexity in the pathophysiological mechanism responsible for DCS. However, during the course of experimentation, several factors advocates for the use of injected bubbles. Firstly, decompression induced bubbles may not necessarily be displayed superficially, but evolve deep within the tissue and thus be incapable of verification. This would increment the amount of animals necessary to conduct statistical comparisons and the number of animals would further be augmented since a pronounced decompression induced impact would claim a higher rate of casualties, which would prolong the experimentation phase and constitute ethical considerations. Secondly, decompression induced bubbles as well as injected bubbles must obey Fick's first law of gas diffusion (31, 32, 98). Therefore once formed, bubbles will equalize with the surrounding tissue and balance the partial pressures and fractions of the bubble gas content with those present in the tissue thereby assuring comparability of injected bubbles versus DCS bubbles. Thirdly, injected bubbles may be larger than DCS bubbles and therefore seem incomparable since larger bubbles show a tendency towards faster bubble size changes than small bubbles (79). However, even though an enlarged bubble surface area facilitates gas exchange with the surrounding tissue and thereby increases the net growth and disappearance rate, the overall bubble growth and decay will in accordance to Fick's law of diffusion (31, 32, 98) always rely on differences in partial pressures between bubble and tissue.

In previous reports by Hyldegaard et al. (77, 79) the effect of varies breathing gas mixtures were tested on air bubbles injected into the white matter of the spinal cord and compared to decompression induced DCS bubbles evolved in abdominal adipose tissue of rats. Both experiments (77, 79) underwent a compression and decompression profile from a near saturation air exposure. It was found, that injected bubbles in the spinal white matter behave similar to decompression induced bubbles in adipose tissue disregarding the breathing mixture, and in both experiments O₂ breathing caused a transient bubble growth of 10-100 min (77, 79).

One should always exhibit precaution when drawing clinical recommendations based on animal experimentations in a laboratory. Despite the fact, that the injection model does not comprise intravascular bubble formation, the concomitantly immune response or decompression induced bubbles in tissue, we believe, that the model demonstrates the conditions valid for gas exchange in tissue bubbles during DCS. None the less – occasionally animals do die from DCS in experiment I which suggest that the hyperbaric exposures may well be provocative and previous experiments have shown that rats decompressed directly from sea level to 25 kPa without slow deco will die from aDCS (99). Accordingly in experiment I-IV one cannot completely exclude the

formation of subclinical VGE, tissue bubble formation or immunologic reaction. The comparability of injected bubbles in spinal white matter and abdominal adipose tissue with decompression induced bubbles causing spinal DCS has been further elaborated on by Hyldegaard et al. in (77, 79) and doctoral thesis (99).

Despite of the argumentation above, the injection model contains several variables that need further attention. Changes in bubble size during decompression to the respective barometrical pressures could not be estimated through measurements of bubble volume since the bubble radius was not amenable to verification. Therefore, bubble behavior was approximated through delineation of visible surface area. When decompression to set altitude is initiated bubbles increase in volume in accordance to Boyle's law proportional to the decrease in ambient pressure. However, the proportionality between pressure and volume may not necessarily display an equivalent proportional increase in visible surface area as bubbles grew irregular in shape due to the elasticity of the adipose tissue allowing the expansion and bubbles during expansion may dissect themselves deeper into the tissue. It so follows, that bubbles decompressed to altitude display a seemingly greater variation in size due to the variable changes in visible surface area. Such variation is not seen to a similar degree in the size of the injected bubbles at sea level pressure and adds an uncertainty to our results. To assure visibility of the surface area, bubbles had to be injected superficially into the adipose tissue and if proper identification of the bubble outlines could not be ascertained, such bubbles were rejected from the study. Furthermore, bubble behavior also rely on local alterations in adipose tissue blood flow and O₂ consumption as well as bubble location, because, bubbles located near arterioles will be affected by higher levels of PO₂ than bubbles located far from arteries, veins and capillaries (34). Alteration in vascularisation and perfusion may equally influence the estimated adipose tissue N₂T_{1/2} of 29 min which is determined with a considerable degree of variation (100). Accordingly, inconsistency in bubble behavior is to be expected.

Once decompressed, the rat is not reachable for any corrective attempts while being enclosed in the chamber. For this reason, several bubbles were injected into each animal in order to assure that a minimum of two or more bubbles would be available for proper analysis. It seems that an equal "predetermined number of bubbles" injected into each animal would appear more correct. However, considering the above mentioned variables, it is more desirable with a high amount of injected bubbles rather than a predetermined number. Furthermore, the number of bubbles injected in each animal was also determined by the available surface area of the adipose tissue and in order to assure an appropriate distance between adjacent bubbles as well as a proper separation from blood vessels and intestines.

In our experimental settings the bubble surface tension is unknown since bubble shapes were irregular and not circular, and thus did not allow for a precise calculation of bubble radius. Surface tension will always promote bubble shrinkage and when bubbles become sufficiently small subsequently increase the internal bubble pressure, which will eventually cause the final collapse of the bubble. In manuscript II and III bubbles of similar size containing similar amount of mol gas were used in each experiment in order to assure comparability between groups. However, bubbles were studied at different barometrical pressures and thus the corresponding expansion in bubble volume

would generate an uneven surface tension at the different altitudes.

Therefore, the absence of an estimated surface tension constitutes a degree of insecurity into the comparability between groups. Nonetheless, in all manuscripts (I-IV), once disappearing, most bubbles displayed a tendency towards a linear shrinking phase and did not demonstrate acceleration in bubble disappearance rate until the very last minute before complete bubble resolution. This observation corresponds to the reflections conducted by Goldman (15) on the generalized Young–Laplace equation suitable for gas bubbles in elastic material, since the radius of the injected bubbles is much larger than the thickness of the bubble/tissue interface – see Pic.1 at the front page and Fig. 4 in (15). Accordingly, the influence of surface tension seems confined during the present experimental conditions.

It has been suggested, that the bubble growth observed at altitude, could be attributed to adipose tissue rigidity causing a protracted tissue displacement that would make bubbles *appear* to grow as a consequence of delayed tissue elasticity rather than influenced by gas exchange. However, the effect of Boyle's law is instantaneous, so if protracted displacement was applicable, the tissue would have to maintain a higher internal pressure of the bubble than the corresponding external ambient pressure. This would increase the partial pressures of the bubble gas content and promote bubble shrinkage rather than bubble growth, the more so if partial pressures of the gases in question are higher in the bubble than in the surrounding tissue and blood. Furthermore, if changes in bubble volume were influenced by delayed tissue displacement rather than gas exchange, it seems reasonable to assume, that all bubbles would display a similar behavior disregarding the partial pressures of the gas content in bubble and tissue since all bubbles in all experiments are injected into the adipose tissue under exact same conditions. This argument was contradicted by the results from experiment II, where at 25 kPa 1/3 of the O₂ bubbles only displayed a shrinking phase without a transient growth phase while 2/3 of the O₂ bubbles showed a transient growth phase after which bubbles disappeared, and in our previous report air bubbles at 25 kPa in non-preoxygenated rats (group 1 in (39)) demonstrated a continuous growth phase during the entire observation period without disappearing. It hereby follows, that adipose tissue is a tissue with a high degree of elasticity (i.e. low tissue tension) and is free to displace itself under the Mylar and Polyethylene membrane. Therefore, on behalf of the deduction above, once pressure is held constant, bubble size changes must primarily rely on partial pressure differences of the involved gases, tissue blood perfusion and Fick's law of diffusion.

In the present experiments, the uncertainties mentioned above are accommodated by a sufficient number of injected bubbles and animals used which substantiate the statistical comparisons. The fact that each of the experimental groups presented a rather uniform behavior of bubble size changes supports the validity of the method.

Metabolic gases and water vapor

Manuscript II and III:

Bubble kinetic models suggest, that O₂, CO₂ and water vapor will contribute significantly to tissue bubble volume and growth when lowering the ambient pressure during altitude exposures (31, 36, 37). In recent studies we found, that air bubbles injected into adipose tissue of rats decompressed from sea level and

studied 71 kPa (38) or 25 kPa (39) (~2,900 and ~10,376 m above sea level) during O₂ breathing displayed increasing growth and disappearance times when lowering the ambient pressure from 101.3, 71 (38) to 25 kPa (39). At both sea level pressure and 71 kPa bubbles would eventually disappear (38) while bubbles at 25 kPa stabilized without disappearing (39). This difference in bubble decay and stabilization at 101.3, 71 and 25 kPa was ascribed to the contribution of metabolic gases and water vapor to bubble volume at hypobaric exposures. Therefore, the aim of manuscript II and III was to study the effect of O₂, CO₂ and water vapor during low pressure exposures using two different experimental settings in order to establish:

1. the contribution of metabolic gases and water vapor to bubble growth and decay at 25 kPa altitude exposure
2. an ambient pressure altitude threshold for air bubble decay and stabilization in rat adipose tissue

The first aim was tested by injecting of O₂ bubbles into rat adipose tissue depleted from N₂ after which bubbles were studied at sea level or 25 kPa during continued O₂ breathing. Rats were denitrogenated by means of a 3-h period of O₂ pre-breathing leading to almost complete N₂ elimination due to a N₂ tissue half-time (N₂T_{1/2}) of 29 min in adipose tissue of rats during O₂ breathing, measured by means of radioactive Xe¹³³ washout, since the tissue perfusion is 0.105 ml blood x g⁻¹ x min⁻¹ and the partition coefficient (λ) for N₂ between 85% lipid and blood is 0.066/0.0148 for rat abdominal adipose tissue (14, 100). At the time of O₂ bubble injection eight tissue halftimes have elapsed (8 N₂T_{1/2} = P_{tissue}N₂ < 0.4%) and in the group decompressed to altitude more than nine tissue halftimes have elapsed (9 N₂T_{1/2} = P_{tissue}N₂ < 0.2%). Accordingly, by assuring almost complete lack of N₂ in adipose tissue, changes in bubble size would not depend on N₂. We found, that O₂ bubbles at altitude demonstrated a significantly slower disappearance rate when compared to O₂ bubbles at sea level, and significantly more O₂ bubbles at altitude displayed a transient growth phase (18 of 27 bubbles initially grew for a period of 2-40 min) as compared to sea level at which no growth was observed.

The second aim was tested by injecting air bubbles in rat adipose tissue followed by decompression to the respective altitudes of 60, 47 or 36 kPa (~4,205, ~6,036 and ~7,920 m above sea level). When switched to O₂ breathing (F_iO₂ = 1) just before decompression, P_{tissue}N₂ is reduced through exhalation at a N₂ tissue half-time (T_{1/2}N₂) of 29 min. Assuming that the P_{tissue}N₂ equilibrates with the P_{bubble}N₂, that there is no pulmonary diffusion limitation or physiological shunt, then the P_{bubble}N₂ would be equal P_{Alveolar}N₂ (34). Subtracting the alveolar partial pressures of O₂, CO₂ and water vapour the P_{bubble}N₂ equals = 76 kPa (101). When the rat is decompressed to 60 kPa in 2 min and assuming the same prerequisites as mentioned above, the P_{Alveolar}N₂ will be approximately 42 kPa ((60 kPa – 6.3 kPa (H₂O)) x 0.79). Disregarding the short period of O₂ breathing during decompression (~0 T_{1/2}N₂), the P_{tissue}N₂ supersaturation will be approximately 34 kPa (76 kPa – 42 kPa). Similarly, when decompressed to 47 kPa in 18 min the P_{Alveolar}N₂ is 32 kPa ((47 kPa – 6.3 kPa (H₂O)) x 0.79). The period of O₂ breathing is close to 1/2 T_{1/2}N₂ and hence, the P_{tissue}N₂ supersaturation will be approximately 33 kPa ((76 – 32) x 0.75; since 1/2 T_{1/2} = 25%). Assuming the same prerequisites applicable at 36 kPa, the period of O₂ breathing is close to 1 T_{1/2}N₂ causing a P_{tissue}N₂ supersaturation of approximately 27 kPa. The observed similar behav-

our in bubble growth time, rate and ratio at 60, 47 or 36 kPa ambient pressure may partly be explained by the same degree of $P_{\text{tissue}}N_2$ supersaturation (difference from 1 to 7 kPa). However, significantly more injected micro air bubbles stabilized without disappearing at 36 kPa as compared to 60 or 47 kPa ambient pressures despite the smaller $P_{\text{tissue}}N_2$ supersaturation at 36 kPa. This observation, along with the observed growth and reduced disappearance rate of O_2 bubbles 25 kPa in N_2 depleted tissue may be explained by several mechanisms present during decompression to altitude:

1) The immediate effect of decompression to altitude is bubble expansion according to Boyle's law thereby increasing the bubble surface area. Enlarged bubble surface area creates a larger bubble to tissue interface, facilitating gas diffusion across the bubble wall (31) which for a given diffusion gradient, causes a higher flux between bubble and tissue (31). In accordance with Fick's first law of diffusion (31, 32, 98) and the greater solubility and permeability (i.e. the product of the diffusion coefficient and solubility coefficient (14)) of O_2 than that of N_2 in a lipid tissue, a larger tissue surface interface will facilitate the diffusion of O_2 into the bubble at altitude.

2) Since the steep part of the O_2 dissociation curve is reached sooner in hypobaric than in normobaric conditions, the Bohr effect (when the $P_{\text{arterial}}O_2$ is below 12-13 kPa) promotes the exchange of O_2 from blood to tissues by right shifting the oxyhemoglobin dissociation curve.

3) As the $P_{\text{arterial}}O_2$ is reduced during decompression, it is conceivable, that the vasoconstrictor effect of O_2 is more pronounced at 101.3 kPa than at altitude, which would favour the microcirculation and thereby enhance the O_2 supply to tissues at altitude.

4) The "inherent unsaturation" (33) between the sum of alveolar gas partial pressures and the total gas tension in venous blood is at a difference of 7.8 kPa and known as the "oxygen window" (102). The pressure gap or inherent unsaturation will always promote tissue bubble shrinkage. However, during pressure changes in the hypobaric range, $P_{\text{alveolar}}O_2$ and $P_{\text{tissue}}O_2$ falls in proportion to the reduced P_{iO_2} while PH_2O and $P_{\text{tissue}}CO_2$ remains constant, thus impairing the effect of the oxygen window concomitantly to reduction in ambient pressure (34). With reference to the measured mean $P_{\text{tissue}}O_2$ (see Table 3 and Fig. 7) in manuscript III **the proportionality of $P_{\text{tissue}}O_2/P_{iO_2}$ at 60, 47 and 36 kPa** can be calculated since 1 kPa equals 7.5 mmHg; 24 kPa/60 kPa = **0.4**; 19.47 kPa/47 kPa = **0.41**; 13.2 kPa /36 kPa= **0.37**. Further, during sustained O_2 breathing the amount of dissolved tissue O_2 in the bubble region will increase and eventually decrease the O_2 window between bubble and tissue as deduced by Foster et al. (32).

5) When reducing the ambient pressure, the amount of mol O_2 transported to tissues does not decrease proportional to the reduction in P_{iO_2} because of hemoglobin. However, in accordance to Boyles law, the volume (ATPS; ambient temperature and pressure, saturated) increases inversely proportional to ambient pressure. Therefore, the volume of O_2 (ATPS) supplied to the tissues will be greater at lower ambient pressure (31, 37). Accordingly, at 25 kPa, the volume of O_2 (ATPS) will increase by a factor of 3.7 (0.92 x 101.3: 25) despite the amount of O_2 (STPD; stand-

ard temperature and pressure, dry) carried to the tissue is reduced by approximately 8% (see deduction in (103)) in comparison to O_2 breathing at sea level.

In manuscript III and (39), the stabilization observed at 36 kPa (III) and 25 kPa (39) must rely not only on the argumentation above (1-6) but also on the N_2 supersaturation promoting an influx of N_2 from tissue to the bubble. This will dilute the O_2 content in the bubble and enhance further diffusion of O_2 from arterial blood to bubble causing bubble growth. As previous deduced in (39), an O_2 partial pressure difference between arterial blood and bubble of $0.8 + P_{\text{bubble}}N_2$ kPa exist sustaining the growth and stabilization. During continues O_2 breathing N_2 will eventually diffuse from the bubble ($T_{\frac{1}{2}}N_2$ of 29 min (100)) driven by the N_2 partial pressure difference between bubble, tissue and blood. This will increase the PO_2 inside the bubble and promote an outward diffusion of O_2 to the surrounding metabolizing tissue. At the end of the observation period $P_{\text{bubble}}N_2$ and $P_{\text{tissue}}N_2$ will be close to zero since up to 8 $N_2T_{\frac{1}{2}}$ have elapsed ($8 N_2T_{\frac{1}{2}} = P_{\text{tissue}}N_2 < 0.4\%$) and the O_2 partial pressure difference between $P_{\text{arterial}}O_2$ and $P_{\text{bubble}}O_2$ is reduced towards 0.8 kPa (39). At this point, more O_2 is lost to the surrounding metabolizing tissue than what is received from the arterial blood explaining bubble shrinkage. CO_2 has a high blood and tissue solubility (14) and small PCO_2 difference between arteries and veins relative to $P_{\text{arterial/tissue}}O_2$ (14). It is therefore conceivable that CO_2 constitute a negligible influence on changes in bubble volume. However, during anaerobic metabolism such as during blockage of circulation e.g. due to gas embolism, CO_2 liberation from bicarbonate stores in blood and tissue may reach high levels that could contribute significantly to bubble volume (34). In III, $P_{\text{tissue}}O_2$ was evaluated by a Licox™ catheter. We found that $P_{\text{tissue}}O_2$ varied from 24 to 13 kPa when decreasing ambient pressure from 60 to 36 kPa supporting the hypothesis that $P_{\text{tissue}}O_2$ remains relative stable compared to the greater reduction of P_{iO_2} (31, 36, 37). However, it should be noted that Licox™ $P_{\text{tissue}}O_2$ measurements were encumbered by a degree of inaccuracy.

The results indicate, that metabolic gases, O_2 in particular, and water vapor in addition to N_2 contribute to bubble growth during hypobaric exposures and that the threshold altitude for air bubble decay or stabilization is between the interval of 36-47 kPa of altitude (~6,036 and ~7,920 m above sea level). The threshold found, is in agreement with a previous report by Webb et al. (104) demonstrating an increase in the formation of VGE and symptoms of aDCS at altitudes higher than 44 kPa ambient pressure. Furthermore, the fraction of N_2 in air bubbles will increase the growth, and prolong the stabilization and disappearance phase as compared to O_2 bubbles in N_2 depleted tissue.

Perfluorocarbon emulsions

Manuscript I:

In previous reports, Hyldegaard et al. have shown that decompression induced N_2 bubbles in adipose tissue (79) and micro air bubbles injected into the white substance of the spinal cord (77), will initially grow for a period of 10 to more than 100 minutes, then shrink and disappear during O_2 breathing at sea level. This undesirable initial growth during O_2 breathing has been explained by a minor flux of N_2 out of the bubble than the concomitantly flux of O_2 into the bubble mainly as a result of the greater transport capacity of O_2 than N_2 in blood (14).

Accordingly, we speculate that combined O_2 breathing and PFC infusion could promote the growth of extravascular bubbles

upon decompression to sea level due to the increased O₂ supply by PFC. In keeping with PFC's high capacity for dissolving N₂, it also seems plausible that the initial bubble growth seen during O₂ breathing could be either reduced or even eliminated due to the greater transport capacity of N₂ in PFC enhancing the N₂ desaturation. Therefore, the aim in manuscript I was to study the effect of PFC (Oxygent[®], Alliance Pharmaceutical, US: *perflubron*; T_{1/2} in blood 4-8 h (105)) on tissue air bubbles in rats decompressed to sea level from a hyperbaric air dive using three experimental groups breathing either 1) air, 2) O₂ or 3) O₂ combined with PFC infusion.

When decompressed to sea level, bubbles in all three groups presented an initial growth phase. This observation can be explained by the influx of N₂ from the surrounding tissue, since decompression from 385 kPa to 101.3 kPa during air breathing causes a N₂ tissue supersaturation of approximately 170 kPa (106) explaining the overall bubble growth. During continued air breathing in group 1) all bubbles grew for about 27-152 min, after which they remained stable or began to shrink slowly indicating equilibrium between growth provoking factors (i.e. tissue supersaturation) and shrinkage promoting influences such as the O₂ window effect (34, 35) and overpressure in the bubble caused by surface tension and tissue elastic recoil. Eventually the P_{tissue/bubble}N₂ will equilibrate with the P_{Alveolar}N₂ and P_{arterial}N₂ and the main driving force will further bubble elimination caused by the O₂ window effect and overpressure in the bubble as outlined above. When rats are switched to O₂ breathing in the remaining groups, bubbles in group 2) were found to grow for 16-126 min similar to previous publications (77, 79). During O₂ breathing the transient growth phase can in addition to influx of N₂ from the surrounded supersaturated tissue be explained by influx of O₂, due to 1) blood's ability to carry more dissolved O₂ to the tissue than it can concomitantly remove N₂ mainly caused by hemoglobin when the PO₂ in the tissue is 12-13 kPa; at higher PO₂ by the difference in solubility coefficients (0.022 ml gas x ml blood⁻¹ x atm⁻¹ for O₂, 0.0148 ml gas x ml blood⁻¹ for N₂), i.e. at equal partial pressure differences, blood will carry more dissolved O₂ to the tissue than it can concomitantly remove N₂; and 2) by the greater O₂ permeability in the lipid tissue than of N₂ (13, 14). Consequently, the enhanced flux of O₂ into the bubble will 3) dilute the N₂ in the bubble favoring further diffusion of N₂ from the supersaturated surrounding tissue into the bubble. This effect is enhanced by the increasing fraction of O₂ in the bubble but wanes as the tissue is desaturated for N₂. Thus, as the P_{bubble}O₂ increases the O₂ gradient from bubble to tissue increases and concomitantly the O₂ gradient from blood to bubble decreases. Eventually, the total loss of O₂ and N₂ from the bubble will exceed the influx of O₂ and N₂, and the bubble will shrink as O₂ diffuses to the surrounding metabolizing tissue and N₂ will be exhaled because of the increased O₂ window (34). Four bubbles only displayed a stabilization phase maintaining their augmented size without disappearing during the observation period. This observation corresponds to previous reports (38, 77, 79), at which bubbles equally were found to behave variable and unpredictable during O₂ breathing.

When combining O₂ breathing with PFC infusion in group 3), bubble growth rate increased, however the growth ratio was significantly smaller than during air breathing and bubbles grew for a shorter period of about 15-53 min. Furthermore, bubbles presented a significantly faster disappearance rate than during both air breathing and O₂ breathing alone. Assuming an equal O₂ metabolism and consumption in the adipose tissue of all three experimental groups, the initial bubble growth and subsequent

shrinkage observed in group 3), may be explained by the same prerequisites as during O₂ breathing alone. Accordingly, the faster growth rate seen in the PFC group, must be ascribed to, 1) the increased O₂ supply by PFC, leading to increased O₂ flux into the bubble, thereby diluting the N₂ in the bubble and increasing the gradient for diffusion of N₂ from the surrounding supersaturated tissue to the bubble. Further, 2) the observed initial growth may be attenuated, since O₂ breathing and PFC infusion were administered immediately after decompression followed by an approximately 8-15 min period of bubble injection, resulting in a minor reduction of N₂ tissue partial pressure (T_{1/2}N₂ 29 min (100)) before bubble observations were initiated. The faster net disappearance rate must be caused by, 3) the greater transport capacity of N₂ in blood by the intravascular PFC enhancing the N₂ tissue desaturation. Further, 4) since PFC infusion increases the intravascular plasma volume of about 1 ml, it seems plausible that the volume expansion could improve the peripheral micro circulation and thereby alleviate the negative effect of O₂ induced vasoconstriction, although the 1 ml volume of PFC infusion represents less than 5% of the total accumulated saline infusion (5-6 ml) during the experiment and estimated total rat blood volume of 16-23 ml giving a rat weight of 250-350 gram (107, 108).

In conclusions, combined O₂ breathing and PFC infusion significantly increased bubble disappearance rate when compared to both air and O₂ breathing alone adding further support to the efficient use of treating DCS with PFC emulsions. Although combined O₂ breathing and PFC infusion did not eliminate the initial transient growth phase and even caused a significantly faster growth rate than during air breathing, there was no differences in growth rate, growth time or growth ratio when compared to O₂ breathing alone. Accordingly, the results do not support the hypothesis that combined O₂ breathing and PFC infusion enhances the initial bubble growth as compared to O₂ breathing alone, and therefore we find no reservations with respect to the use of PFC infusion during DCS when compared to standard O₂ breathing.

Manuscript IV:

Whether PFC emulsions equally constitute therapeutic properties during aDCS as observed during DCS from diving have not been demonstrated and in vivo observations of extravascular bubble size changes in animals decompressed from sea level to hypobaric exposures during O₂ breathing have not been reported before. Therefore, the aim in manuscript IV was to study the effect of PFC (Oxygent[®], vapor pressure at 37°C = 1.4 kPa/10.5 torr (65)) on tissue air bubbles in rats at 25 kPa altitude exposure during O₂ breathing and compared to a control group breathing O₂ alone from a previous report with exact same experimental conditions (39). Since combined PFC infusion and O₂ breathing showed significantly faster bubble disappearance rate of tissue bubbles at sea level in I, our primary endpoint was from a clinical point of view an equally enhanced rate of bubble resolution at altitude.

In manuscript IV, we used the same dose and way of administration of PFC as in manuscript I, and it should be expected that PFC would equally favor tissue bubble disappearance at altitude as observed at sea level through an increased transport capacity of N₂ by means of PFC circulating in blood (40, 42). On the other hand, in keeping with the contribution of metabolic gases and water vapor to bubble volume at altitude as demonstrated in our previous report (39) and in manuscript II and III, combined with the greater solubility and permeability of O₂ in a lipid tissue than that of N₂ (14), it is conceivable, that the increased O₂ transport

capacity by PFC could also favor bubble growth and subsequent stabilization at hypobaric conditions.

When decompression to 25 kPa was reached, all air bubbles in both the experimental PFC group and the control group (39) initially grew, then stabilized or began to shrink slowly. When the rat is switched to O₂ breathing just before decompression to altitude, the P_{tissue}N₂ is reduced through exhalation at a tissue T_½N₂ of 29 min (100). Accordingly, the 36-min period of O₂ breathing during decompression is close to 1¼ T_½N₂ causing a P_{tissue}N₂ supersaturation of approximately 30 kPa (39) at altitude. Consequently, N₂ from tissue will diffuse to the bubble, diluting O₂ in the bubble thereby furthering additional diffusion of O₂ from arterial blood to bubble, explaining the overall bubble growth.

However, in previous experiments, both air (39) and O₂ bubbles in manuscript II were found to grow and stabilize while at 25 kPa ambient pressure, despite complete N₂ depletion from the tissue through preoxygenation. Further, under similar experimental conditions, a threshold altitude of tissue bubble stabilization or decay was found to be in the interval between 47-36 kPa in manuscript III. The effect was ascribed to the contribution of metabolic gases, O₂ in particular, and water vapor and is consistent with bubble kinetic models (31, 36, 37). Therefore, the growth observed in the manuscript IV must also rely on influx of O₂, CO₂ and water vapor from the surrounding tissue. Eventually, N₂ will diffuse from the bubble to the blood at a decreasing rate as P_{bubble}N₂ decreases (T_½N₂ 29 min (100)) promoting bubble shrinkage. However, most bubbles maintain their size in the latter part of the observation period indicating equilibrium between O₂ gained from the blood and O₂ lost to the surrounding tissue, since, up to 8 N₂T_{1/2} have elapsed and P_{bubble}N₂ and P_{tissue}N₂ therefore will be close to zero (8 N₂T_{1/2} = P_{tissue}N₂ < 0.4%). Only 2 bubbles within the PFC treated animals disappeared during the observation period while no bubbles disappeared in the control group (39).

When the group administered PFC is compared to the control group breathing O₂ alone from our previous report (39), bubble growth time was significantly longer during O₂ breathing alone when compared to rats receiving PFC. There were no other differences regarding growth rate, growth ratio, growth time or net disappearance rate between the present experimental data in manuscript IV and the previous data (39). Accordingly, it is concluded, that the present results do not support the hypothesis that PFC emulsions enhance the initial bubble growth at altitude when compared to O₂ breathing alone. However, nor do the results support our primary endpoint, that combined PFC infusion and O₂ breathing increase bubble disappearance rate at 25 kPa altitude pressure. The lack of effect may be explained by the increasing contribution of metabolic gases and water vapor to the bubble content during hypobaric exposures.

It is an obvious limitation in manuscript IV, that P_{tissue}O₂ levels were not measured and it would equally have been favorable to substantiate the effect of PFC in both manuscript I and IV by additional parameters, such as measurements of PO₂ and PN₂ in arterial and venous blood, PFC levels in or near the vasculature of the adipose tissue and plausible changes in vasoconstriction and dilation along with estimates of blood flow rate. However, in manuscript I, P_{tissue}O₂ levels measured by Licox catheter were significant greater during combined O₂ breathing and PFC infusion than during air breathing, but not quite significant elevated when compared to O₂ breathing alone (0.1 > P > 0.05). Despite the lack of significant effect, the increased levels of P_{tissue}O₂ during PFC

administration, gives an indication of the gas transportation properties conducted by PFC.

Nitric oxide

Manuscript IV:

Previous reports (66-69), describing the beneficial effect of NO donors as a preventive matter against DCS from diving, have studied intravascular gas formation or survival rate. Since no reports have been published describing therapeutic properties of NO donors on extravascular tissue bubbles, the aim of manuscript IV was to study the effect of NO a donor on air bubbles injected into adipose tissue and decompressed to a hypobaric altitude exposure during O₂ breathing using two experimental groups. The first group received ISMN (isosorbide-5-mononitrate) while the second group received combined ISMN and PFC (Oxygent®) infusion in order to clarify any synergetic effect. The two treatment modalities are compared to a control group from a previous report (39), at which rats breathing O₂ alone were decompressed to a 25 kPa altitude exposure under exact same experimental conditions.

Previously, Wisløff et al. (68) have demonstrated that a long acting NO donor (isosorbide-5-mononitrate, ISMN; p.o. 65 mg/kg; T_½ 268 ± 40 min (85)), administered 30 min prior to a simulated air dive significantly reduced VGE formation and improved survival rate of rats anaesthetized upon arrival to sea level. Accordingly, in the present experiment, the same dose and way of administration as used in (68) was replicated and ISMN infused 30-40 min prior to decompression to altitude.

It seems conceivable, that if the beneficial effect of ISMN on DCS can be entirely ascribed to elimination of nuclei precursors from the endothelium wall, the injected air bubbles in the present experiment will supposedly behave similar to the injected air bubbles in our previous report (39) despite the ISMN administration since bubbles of the present experiment are located in the extravascular compartment. However, if bubble elimination can be ascribed to an increased tissue perfusion rate due to the increased blood flow rate (80) with arteriolar dilation (81) caused by NO, the influence on tissue bubbles could be two fold. Firstly, since the presence of N₂ in injected bubbles and tissue has shown to significantly extend bubble growth and stabilization (39, 103), the enhanced blood flow rate could improve denitrogenation from bubble and tissue and thereby increase the disappearance rate. Secondly, enhanced blood flow rate could increase the O₂ supply to tissue, and in keeping with the increased contribution of metabolic gases and water vapor to bubble growth at altitude (31, 36, 37), combined with the greater transport capacity of O₂ in blood as well as greater blood solubility and permeability of O₂ in lipid tissue than that of N₂ (13, 14), it seems conceivable, that ISMN could generate additional unwanted growth and stabilization of tissue bubbles at hypobaric conditions.

When the experimental groups receiving ISMN and combined ISMN and PFC are compared to the control group breathing O₂ alone from our previous report (39), bubble growth time was significantly longer during O₂ breathing alone when compared to rats receiving ISMN. However, the overall bubble growth and decay regarding growth rate, growth ratio or net disappearance rate do not display any other significant differences when compared to the control group (39). Apparently, neither ISMN alone or in combination with PFC share the same therapeutic properties on tissue bubbles at altitude as observed separately on intravascular bubble formation (66-68) and tissue bubbles (I) (106) at

sea level upon hyperbaric exposures. Accordingly, it seems reasonable to assume, that enhanced gas exchange as a consequence of alteration in blood perfusion rate does not constitute a prevailing mechanism at 25 kPa ambient pressure. Hypobaric hypoxia is known from mountain climbing to cause vasodilatation in tissues and increase blood flow-, ventilation- and heart rate (109, 110), and therefore it could be argued, that enhanced blood flow and vasodilatation induced by NO donors may constitute a negligible effect at altitude during low levels of $P_{\text{arterial}}\text{O}_2$. However, as deduced in *equation 3* in (103), when breathing 100% O_2 at 25 kPa altitude, $P_{\text{arterial}}\text{O}_2$ will not reach hypoxic levels and thus cannot explain a plausible compromised effect of exogenous NO.

In the present study, it is an obvious limitation that DCS bubbles in the intravascular compartment were not studied since NO administration showed no significant influence on the overall growth and decay of tissue bubbles when compared to the control group (39). Therefore, the present results cannot omit the possibility, that the reported beneficial effect of NO donors on DCS from diving (66-68) relies on a nuclei demise. However, during combined PFC and ISMN infusion, bubble behavior showed no significant differences when compared to both ISMN or PFC administration alone, nor were there any major differences in the overall growth and decay when all three experimental groups were compared to the control group (39). Accordingly, since neither PFC infusion alone (IV) or in combination with ISMN showed the same therapeutic abilities on tissue bubbles at altitude as observed during PFC infusion at sea level, then the lack of effect may be ascribed to a predominant contribution of metabolic gases and water vapor (31, 32, 36, 37) to the bubble volume as well as an impaired effect of the O_2 window (34) at low pressure exposures.

Manuscript V:

Whether NO donors affects protection against potential autochthonous bubble formation in CNS (28-30) as observed on intravascular bubble formation (66-68) during DCS has not been reported. Therefore, the aim of the manuscript V was to test the therapeutic properties of NO donors (ISMN, isosorbide-5-mononitrate; GTN, nitroglycerine) on spinal cord conductivity during DCS evolved from a hyperbaric air exposure. It seems conceivable that if NO donors reduce the intravascular bubble formation through elimination of endothelial micro nuclei precursors, then NO donors administered before a dive may increase the survival rate and demonstrate a protecting effect on the SEP's in case the arterial emboli (24), venous infarction (25) or complement activation (26, 27) are the primary mechanisms responsible for DCS in CNS. However, if autochthonous bubbles (28-30) are the primary cause for DCS in CNS, reduction in nuclei density by NO donors may decrease the intravascular bubble formation while injuries in CNS may persist. On the other hand, if the beneficial properties of NO donors on DCS relies on upgraded gas exchange due to augmented tissue perfusion, then the short period of hemodynamic changes caused by NO donors (85, 87) may constitute a narrow therapeutic interval from administration to the decompression induced insult.

Accordingly, in the present experiment, a hemodynamic alteration as a possible mechanism for preventing DCS in CNS was tested by administration of both ISMN in group 4) and GTN in group 5) and 6) during the dive; see Experimental groups in the Methods section. If increased gas exchange enhances the N_2 elimination during the decompression phase as a consequence of alterations in blood flow, it seems reasonable to assume, that an

equivalent N_2 uptake in tissues ought to commensurate during the preceding dive and therefore, in order to promote the beneficial effect, NO donors should be dispensed just prior to decompression. In a previous report by Møllerløgken et al. (66) of DCS in a swine model, it was found, that GTN significantly decreased the intravascular bubble formation when given at a dosage twice the recommended in humans during a saturation dive to 500 kPa (40 msw) subsequent to a linear decompression phase of 2 h. Accordingly, in group 4-6) the NO donors were administered 3-8 min before initiation of decompression and at a high dose that would inflict a hemodynamic impact during the decompression procedure (85, 87). However, when compared to the control group, NO donors in group 4-6) showed no protective effect on survival rate or spinal cord conductivity when administered immediately before decompression. On the contrary, administration of a high dose of GTN in group 5) resulted in significantly faster SEP disappearance and showed a tendency towards shorter survival time than the control group while a lower dose of GTN in group 6) also showed a tendency of faster SEP disappearance though this was not significantly different. Further, administration of ISMN in group 4) showed no deviant effect on SEP disappearance or survival time when compared to the control group, despite the dose and way of administration for ISMN causes a peak pulse pressure effect after $10.5 \text{ min} \pm 4.7$ (85).

In the saturation swine model by Møllerløgken et al. (66), the GTN infusion significantly elevated the heart rate and reduced MAP, though, it could not be determined, whether the protective effect of GTN was attributed to hemodynamic changes or removal of micro nuclei precursors. Similarly in the present experiment, it cannot be excluded, that NO donors administered prior to decompression could initiate a demise of pre-existing gas nuclei. However, if that is the case, it seems evident, that removal of nuclei implies a therapeutic window exceeding the present interval from NO donor administration to the decompression induced insult in group 4-6). Since the hemodynamic effect of NO donors wears off within min (85, 87) when administered at a clinical dose and since the regeneration time for a depleted nuclei population is 10-100 h (111), any protective effect of NO donors when administered before a dive advocates for a decrease in nuclei density as the predominant factor rather than conditioned by flow limitations. In a previous report by Dujic et al. (67), divers received 0.4 mg GTN by oral spray 30 min prior to both a 30 min open water dive to 30 msw and a 80 min hyperbaric air dive to 18 msw followed by a decompression phase of respectively 6 and 9 min. Further, in a previous report by Wisløff et al. (68), non anaesthetized rats were administered ISMN 65 mg/kg by gastric intubation 20 h or 30 min prior to a 45 min hyperbaric air dive to 700 kPa after which they were decompressed to surface in 12 min. In both divers and rats, NO donors significantly decreased the intravascular bubble formation as well as increased the survival rate in rats, an effect ascribed to a possible reduction of pre-existing gas nuclei. In the present experiment, we replicated these intervals from administration of NO donors to the decompression induced impact, hence group 2) and 3) were administered ISMN and GTN respectively 5-10 and 30 min before compression; see Experimental groups in the Methods section. None the less, just like group 4-6), administration of GTN in group 3) showed a tendency towards shorter survival and faster SEP disappearance although dispensed at a high dose, while administration of ISMN in group 2) had no deviant effect on survival time or spinal cord conductivity despite a $T_{1/2}$ for ISMN of $268 \pm 40 \text{ min}$ (85).

In the NO manuscripts IV and V, it seems as an obvious limitation than only changes in MAP were registered. Both experiments would benefit from a more detailed collection of data, monitoring the effect of NO on gas tensions and circulatory parameters i.e., blood perfusion rate, adipose tissue- and spinal cord perfusion rate, changes in cardiac output, P_{N_2} in venous blood, PO_2 in adipose tissue and the white mater of the spinal cord, NO levels in or near the vasculature of the adipose tissue and the spinal cord etc.

Although blood flow was not directly measured, NO donors are known from the literature, based on both human and animal experimentation, to cause venous dilation with sequestration of blood from the central arterial circulation to the capacitance bed, thereby reducing cardiac preload (80, 112, 113) and increasing the peripheral blood flow rate in the extremities (82-84). Whereas the veins are maximal dilated with relatively small doses of NO donors the arterioles or resistance vessels dilate with high amounts (80, 113) and with GTN influencing the systemic vascular resistance far more potent than ISMN (87).

During DCS, gas bubbles primarily evolve within the venous system (23). It therefore seems plausible, that the NO donor induced pooling of blood to the venous circulation combined with arteriole dilation and increased blood flow may promote an even faster off-gassing of N_2 from the supersaturated tissue to the venous blood. If this is the case, it could be speculated, that NO donors may have a contradictory effect during DCS from diving since enhanced N_2 liberation in combination with a rapid decompression phase could increase the amount of harmful gas bubbles in venous blood. If the resulting bubble burst overloads the pulmonary ability of excretion then NO donors may potentially aggravate the DCS symptoms. On the other hand, it could be argued that enhanced N_2 liberation from tissues to venous blood in combination with an extended decompression phase could improve the pulmonary excretion during the decompression phase thus reducing the ratio of N_2 supersaturation ($P_{tis-sue}N_2/P_{ambient\ pressure}$) upon arrival at sea level. This could explain why administration of a lower dose of GTN combined with a protracted decompression reduced the intravascular bubble formation in the saturation swine model (66), while rats in the present experiment V receiving high doses of GTN combined with rapid decompression showed a tendency towards faster SEP disappearance as well as shorter survival time. Therefore, it could be speculated, that the absence of protective effect of NO donors in experiment V could be entitled to the fast decompression profile causing a DCS impact overriding the therapeutic effect. However, in the previous report by Wisløff et al. (68), rats of similar weight in their control groups were decompressed in 12 min resulting in a median survival range of 27 (2-39) and 19 (8-60) min (group VI and VII in (68)). Since rats in the *Experiment C* of manuscript V (rats breathing spontaneously without being connected to a respirator - see *Evaluation of the SEP model* in the Methods section) survived with a median range of 60 min (2-120) after decompression it appears that the present decompression profile used in manuscript V is no more severe than the profile used by Wisløff et al. (68).

During the present experimental conditions, we found no protective effect of a short or long acting NO donor on spinal cord conductivity or survival time during DCS, regardless of dose and the interval from administration to the decompression induced insult. These results stands in contrast to the previous reports, in which NO releasing agents have shown reduction in VGE and increased survival time during DCS from diving (66-68). Apparently, the present experiment does not support the hy-

pothesis, that NO donors decrease the amount of nuclei precursors. Nor do the results indicate preventive matters as a consequence of hemodynamic alterations. In the contrary, high doses of GTN seemed to compromise both survival time and spinal cord conductivity. These observations may be explained by the effect of NO in combination with a fast decompression profile, speeding up the N_2 release from tissues to the venous vessels and thereby aggravating the DCS impact.

CONCLUSIONS

Metabolic gases and water vapor (manuscript II and III)

In manuscript II the results support bubble kinetic models (31, 36, 37) based on Fick's first law of diffusion, Boyles law and the oxygen window effect (34) and indicates, that metabolic gases, O_2 in particular, and water vapor contribute to bubble volume at an increasing rate when lowering the ambient pressure. Furthermore, in manuscript III the results also indicate that the increasing contribution of metabolic gases and water vapor to bubble volume cause a threshold for bubble stabilization or decay between the altitude of 47-36 kPa (~6,036 and ~7,920 m above sea level). Furthermore, the fraction of N_2 in air bubbles increased the growth and prolonged the stabilization and disappearance phase as compared to O_2 bubbles in N_2 depleted tissue (manuscript II and (39)). Accordingly, we conclude, that N_2 constitute the most important contributor to bubble size changes, while metabolic gases and water vapour contribute to bubble volume and growth when decreasing ambient pressure and that this effect increases significantly above the altitude of 47-36 kPa.

Perfluorocarbon emulsions (manuscript I and IV)

In manuscript I the present results do not support the hypothesis, that combined O_2 breathing and PFC infusion enhance transient bubble growth in adipose tissue as compared to O_2 breathing alone when decompressed to sea level from a hyperbaric air dive. Although PFC infusion elevated the initial growth rate caused by the increased O_2 tension, the combined effect of O_2 breathing and PFC infusion resulted in a significant faster disappearance rate explained by a greater N_2 transport capacity in blood by PFC and enhanced effect of the O_2 window, increasing the rate of N_2 desaturation. When decompressed to altitude in manuscript IV, the present results do not confirm our hypothesis that PFC promotes transient bubble growth in adipose tissue when compared to O_2 breathing alone. Nor do the results comply with the hypothesis that PFC increases bubble disappearance rate at 25 kPa (~10, 376 m above sea level) altitude exposure. Apparently, PFC infusion does not seem to share the same therapeutic properties on tissue bubbles at 25 kPa altitude, as observed on tissue bubbles at sea level. The lack of effect may be explained by the contribution of metabolic gases and water vapor (31, 32, 36, 37) to the bubble volume along with an impaired effect of the O_2 window (34) when lowering the ambient pressure.

Nitric oxide (manuscript IV and V)

In conclusions of manuscript IV, the present results do not support our hypothesis that ISMN independently or in combination with PFC promotes transient bubble growth in adipose tissue during decompression to 25 kPa (~10, 376 m above sea level) altitude when compared to O_2 breathing alone (39). Neither does the result confirm our hypothesis that ISMN independently or in

combination with PFC enhance bubble disappearance rate. Therefore, it is concluded, that the effect of NO on blood perfusion rate is not a prevailing mechanism at 25 kPa altitude exposure. The lack of therapeutic effect may be explained by the increased contribution of metabolic gases and water vapor (31, 32, 36, 37) to the bubble content at low pressure exposures in combination with a decreasing effect of the O₂ window (34). However, when NO donors were dispensed prior to decompression to sea level from a hyperbaric exposure in manuscript V, we found no protective effect of a short or a long acting NO donor regardless of dose and the interval from administration to the decompression induced insult. The result stands in contrast to previous publications (66-68) and advocate against the hypothesis, that NO donors diminishes the density of nuclei precursors. The results also indicate that administration of NO donors is not a beneficial intervention during the present experimental conditions and, on the contrary, seemed to compromise both survival time and spinal cord conductivity. This observation may be explained by the fast decompression profile used in manuscript V, along with NO induced N₂ release from tissues, through alterations of blood flow rate, exceeding the threshold for pulmonary excretion of N₂ thereby causing a fatal pulmonary bubble overload. The observations in experiment V underlines the importance of correct timing and dosing of NO donors in order to obtain the previous reported (66-68) therapeutic effect. This effect may also seem to depend on the actual decompression profile used for the particular diving event.

PERSPECTIVES AND FUTURE STUDIES

Metabolic gases and water vapor (manuscript II and III)

Several cases of aDCS have been reported in U-2 pilots despite a precautionary period of O₂-prebreathing prior to ascent (114-116). In keeping with the present results and bubble kinetic models (31, 36, 37), these examples of aDCS could very well be explained by the contribution of metabolic gases and water vapour to bubble formation, since cabin pressure in U-2 planes during flight mission ranges from 34-32 kPa (~8,839 -9,145 m above sea level) (116) and hence is above the threshold altitude of 36 kPa (~7,920 m above sea level) for bubble stabilization found in the present experiments. Furthermore, in commercial aviation, cruising altitude is usually at the height of 10,000-11,000 m above sea level (~27-23 kPa) while cabin pressure is maintained at 71 kPa (2,900 m above sea level) (117). Thus, the present results are of importance for pilots and passengers, who may develop signs of aDCS upon accidental loss of cabin pressure despite of O₂ breathing and emphasise the necessity of combining O₂ breathing with rapid increase in ambient pressure by descent, since O₂ breathing at 25 kPa altitude caused most bubbles to stabilize regardless of inert gas partial pressure in tissue (39, 103). The results may be particularly important for astronauts during space missions where immediate recompression by descent or treatment in a pressure chamber may not be readily available. We recommend that theoretical models of risk analysis on decompression procedures and low pressure exposures in flight should take these experimental results into consideration.

Perfluorocarbon emulsions (manuscript I and IV)

Conventional treatment of aDCS is O₂ breathing combined with fast descent from altitude, eventually followed by recompression during hyperbaric O₂ breathing (HBO) in a pressure chamber

(118, 119). During DCS after diving the standard treatment is HBO depending on the severity of the symptoms. The purpose of HBO treatment is to reduce bubble size by recompression of the gas phase, improve tissue oxygenation and enhance elimination of dissolved N₂ (118, 119) along with additional positive effects of O₂ such as the ability of being anti-edematous and mitigate the immune response caused by the bubble to blood interface (120). However, HBO treatment may also cause some undesirable effects, such as O₂ induced vasoconstriction (121, 122) and O₂-toxicity (123). If treatment of DCS involves combined HBO and PFC infusion it seems plausible, that the level of threshold for cerebral O₂ toxicity (seizures) as a result of hyperbaric hyperoxia might be reduced due to the elevated levels of O₂ caused by PFC as demonstrated by Mahon et al. (124) and others (48, 125). Previous studies (48, 124) have demonstrated that treatment with PFC at hyperbaric exposures was not as effective as PFC administered at normobaric conditions. Accordingly, it remains to be investigated, whether treatment of DCS with combined PFC infusion and HBO at lower pressures, thus avoiding the risk of O₂ toxicity (126), may be as effective as standard HBO treatment (i.e. 284 kPa US-Navy treatment table 6, (127)). Furthermore, during DCS intravascular bubbles are known to activate several immune mechanisms such as cytokines (26), complement (27) and platelet activation (128). Whether PFC administration during treatment of DCS inflicts therapeutic properties on these immune mechanisms remains to be clarified.

During treatment of DCS, the main objective is a fast bubble resolution without transient bubble growth (129, 130). In previous reports (73, 75, 77, 79), heliox (80:20/50:50) breathing at sea level and during recompression have shown to improve bubble disappearance in lipid and aqueous tissues without the initial bubble growth observed during O₂ breathing. Since the solubility of N₂ in PFC and blood is higher than that of helium (13, 14, 40), it seems that combined PFC infusion and a heliox breathing mixture could be beneficial on bubble resolution in lipid and aqueous tissues and in the treatment of DCS. This has yet to be evaluated by future experiments.

Nitric oxide (manuscript IV and V)

NO donors are well known from clinical settings and cause only minor side effects (131). Therefore, considering the previous reported beneficial effect of NO donors during DCS from diving (66-68), it seems, that NO donors as a prophylactic intervention against DCS could easily be implemented. However, considering the present results of manuscript V, it appears that future studies are necessary in order to establish the optimal dose of NO donors on survival and spinal cord conductivity during different decompression profiles in diving as well as a deeper insight into possible adverse effects. It has been suggested that NO donors could increase safety in emergency situations such as during submarine escapes (66). Though, in keeping with the tendency of reducing survival time and enhance neurologic deterioration during administration of GTN in the present manuscript V, administration of NO donors prior to rapid decompression seems contraindicated. The pathophysiological mechanism responsible for the neurologic detriments in CNS during DCS is not completely clarified (12) and the role of autochthonous bubbles is still debated (28-30). Therefore, pharmacological intervention with NO donors seems like a mean to a probable understanding of bubble development in the intravascular versus the extravascular compartment. NO is known to inhibit leukocytes and platelet aggregation (132) and since NO may diminish the population of intravascular nuclei precursors

(66-68), NO might be a rewarding way to isolate and study the influence of autochthonous bubbles (28-30) on CNS by alleviating the effect of arterial embolism (24), venous infarction (25) and immunological activation (26, 27) during DCS.

If the main effect of NO is caused by alteration of the endothelium wall (133, 134) and not through enhanced blood flow rate (82-84), it seems arguable that NO could also diminish the amount of intravascular gas formation during decompression to altitude. Since ISMN in manuscript IV caused no adverse effects regarding transient bubble growth or stabilization in tissue when compared to the control group (39), it would be of interest with future investigations testing the effect of NO donors on intravascular bubble formation during aDCS. Although, from an operational point of view, it appears of greater importance to establish whether O₂-prebreathing at ground level in combination with NO donors could speed up the N₂ release from tissues, thereby shorten the costly period of preoxygenation prior to flight missions (135, 136).

SUMMARY

In aviation and diving, fast decrease in ambient pressure, such as during accidental loss of cabin pressure or when a diver decompresses too fast to sea level, may cause nitrogen (N₂) bubble formation in blood and tissue resulting in decompression sickness (DCS). Conventional treatment of DCS is oxygen (O₂) breathing combined with recompression. However, bubble kinetic models suggest, that metabolic gases, i.e. O₂ and carbon dioxide (CO₂), and water vapor contribute significantly to DCS bubble volume and growth at hypobaric altitude exposures. Further, Perfluorocarbon emulsions (PFC) and Nitric Oxide (NO) donors have, on an experimental basis, demonstrated therapeutic properties both as treatment and prophylactic intervention against DCS. The effect was ascribed to solubility of respiratory gases in PFC, plausible NO elicited nuclei demise and/or N₂ washout through enhanced blood flow rate. Accordingly, by means of monitoring injected bubbles in exposed adipose tissue or measurements of spinal evoked potentials (SEPs) in anaesthetized rats, the aim of this study was to, 1) evaluate the contribution of metabolic gases and water vapor to bubble volume at different barometrical altitude exposures, 2) clarify the O₂ contribution and N₂ solubility from bubbles during administration of PFC at normo- and hypobaric conditions and, 3) test the effect of different NO donors on SEPs during DCS upon a hyperbaric air dive and, to study the influence of NO on tissue bubbles at high altitude exposures. The results supports the bubble kinetic models and indicate that metabolic gases and water vapor contribute significantly to bubble volume at 25 kPa (~10, 376 m above sea level) (103) and constitute a threshold for bubble stabilization or decay at the interval of 47-36 kPa (~6,036 and ~7,920 m above sea level) (137). The effect of the metabolic gases and water vapor seemed to compromise the therapeutic properties of both PFC and NO at altitude (138), while PFC significantly increased bubble disappearance rate at sea level (106) following a hyperbaric air dive. We found no protective effect of NO donors during DCS from diving (97). On the contrary, there was a tendency towards a poorer outcome when decompression was combined with NO donor administration. This observation is seemingly contradictive to recent publications and may be explained by the multifactorial effect of NO in combination with a fast decompression profile, speeding up the N₂ release from tissues and thereby aggravating the DCS symptoms.

ACKNOWLEDGEMENTS

I appreciate the opportunity I was given by the Faculty of Health Sciences, University of Copenhagen and Laboratory of Hyperbaric Medicine, The Department of Anaesthesiology, Centre of Head and Orthopedics, Rigshospitalet to work with this thesis. I wish to thank my supervisor Ole Hyldegaard Chief Physician, MD, PhD, DMSc for the encouragement, inspiring discussions and valuable constructive ideas throughout the study as well as inspiring scientific guidance to my work. I am also grateful to my faculty supervisor Hans Hultborn Prof. DMSc for his positive attitude, consistent support and always helpful contributions to this thesis.

I am most thankful to Michael Bering Sifakis senior Hyperbaric Supervisor for invaluable technical assistance and chamber maintenance and to laboratory technician Mr. Ian Godfrey for his help in the manufacture of the glass micropipettes. I also wish to thank associate professor Claire Francesca Meehan for her patient support with setting up the neurophysiologic equipment, assistance with the Spike2 software and the histological preparation as well as Helle Broholm Chief Physician for her assistance with the histological analysis. Thanks are also given to Tina Calundann for her graphical expertise. I warmly thank the doctors and tenders at the Centre of Hyperbaric Medicine for their always positive encouraging attitude, especially Erik Jansen Chief Physician MD, DMSc, Annet Von Brockdorf, Filip Felix Nielsen and Claus Hermansen.

I also wish to express my gratitude to the foundations supporting this thesis; The Lundbeck Foundation, The Laerdal Foundation for Acute Medicine and Rigshospitalets Research Foundation.

REFERENCES

1. M T. Letter to Monsieur. In *Comptes Rendus de l'Académie des Sciences*. Paris: 1885; 20:445-449.
2. Butler WP. Caisson disease during the construction of the Eads and Brooklyn Bridges: A review. *Undersea & hyperbaric medicine : journal of the Undersea and Hyperbaric Medical Society, Inc.* 2004;31(4):445-59. Epub 2005/02/03.
3. Acott C. A brief history of diving and decompression illness. *Journal of the South Pacific Underwater Medicine Society.* 1999;29 (2): 98-109.
4. Elliott DH. Early decompression sickness: compressed air work. *South Pacific Underwater Med Soc J.* 1999;29:28-34.
5. Moir EW. Tunneling by compressed air workers. *J NY Soc Arts* 2. 1896;XLIV (269):567-85.
6. Keays FL. Compressed air illness with a report of 3,692 cases. *Publ Cornell Univ Med College* 1909;2:1-55.
7. Richardson D. Recreational Diving, In: Bennett and Elliott's *Physiology and Medicine of Diving* (5th ed.), edited by Brubakk AO and Neuman TS. Edinburgh, UK: Saunders, 2003, p. 45-55.
8. Elliott DH, Vorosmarti J. An Outline History of Diving *Physiology and Medicine*, In: Bennett and Elliott's *Physiology and Medicine of Diving* (5th ed.), edited by Brubakk AO and Neuman TS. Edinburgh, UK: Saunders, 2003, p. 4-17.
9. Von Schrötter H. *Der Sauerstoff in der Prophylaxe und Therapie der Luftdruckerkrankungen*. Berlin. 1906.
10. Boycott AE, Damant GC, Haldane JS. The Prevention of Compressed-air Illness. *The Journal of hygiene.* 1908;8(3):342-443. Epub 1908/06/01.

11. Stepanek J, Webb T. Physiology of Decompressive Stress, In: Davis JR's Fundamentals of aerospace medicine. 4th ed. Philadelphia: Lippincott Williams & Wilkins; 2008. 46-82 p.
12. Tikuisis P, Gerth WA. Decompression Theory, In: Bennett and Elliott's Physiology and Medicine of Diving (5th ed.), edited by Brubakk AO and Neuman TS. Edinburgh, UK: Saunders, 2003, p. 419-454.
13. Lango T, Morland T, Brubakk AO. Diffusion coefficients and solubility coefficients for gases in biological fluids and tissues: a review. Undersea & hyperbaric medicine : journal of the Undersea and Hyperbaric Medical Society, Inc. 1996;23(4):247-72. Epub 1996/12/01.
14. Weathersby PK, Homer LD. Solubility of inert gases in biological fluids and tissues: a review. Undersea biomedical research. 1980;7(4):277-96. Epub 1980/12/01.
15. Goldman S. Generalizations of the Young-Laplace equation for the pressure of a mechanically stable gas bubble in a soft elastic material. The Journal of chemical physics. 2009;131(18):184502. Epub 2009/11/18.
16. Weathersby PK, Homer LD, Flynn ET. Homogeneous nucleation of gas bubbles in vivo. J Appl Physiol. 1982;53(4):940-6. Epub 1982/10/01.
17. Evans A, Walder DN. Significance of gas micronuclei in the aetiology of decompression sickness. Nature. 1969;222(5190):251-2. Epub 1969/04/19.
18. Vann RD, Grimstad J, Nielsen CH. Evidence for gas nuclei in decompressed rats. Undersea biomedical research. 1980;7(2):107-12. Epub 1980/06/01.
19. James T, Francis R, Mitchell J. Manifestations of Decompression Disorders. In: Bennett and Elliot's Physiology and Medicine of Diving (5th ed.), edited by Brubakk AO and Neumann TS. Edinburgh, UK: Saunders; 2003. P 578-599.
20. Golding FC, Griffiths P, Hempleman HV, Paton WD, Walder DN. Decompression sickness during construction of the Dartford Tunnel. British journal of industrial medicine. 1960;17:167-80. Epub 1960/07/01.
21. Gempp E, Blatteau JE. Risk factors and treatment outcome in scuba divers with spinal cord decompression sickness. Journal of critical care. 2010;25(2):236-42. Epub 2009/08/18.
22. Nishi RY, Brubakk AO, Eftedal OS. Bubble Detection, In: Bennett and Elliott's Physiology and Medicine of Diving (5th ed.), edited by Brubakk AO and Neuman TS. Edinburgh, UK: Saunders, 2003, p. 501-529.
23. James T, Francis R, Mitchell J. Pathophysiology of decompression sickness. In: Bennett and Elliot's Physiology and Medicine of Diving (5th ed.); edited by Brubakk AO and Neuman TS. Edinburgh, UK: Saunders; 2003. P 530-556.
24. Francis TJ, Pezeshkpour GH, Dutka AJ. Arterial gas embolism as a pathophysiologic mechanism for spinal cord decompression sickness. Undersea biomedical research. 1989;16(6):439-51. Epub 1989/11/01.
25. Hallenbeck JM. Cinephotomicrography of dog spinal vessels during cord-damaging decompression sickness. Neurology. 1976;26(2):190-9. Epub 1976/02/01.
26. Ersson A, Linder C, Ohlsson K, Ekholm A. Cytokine response after acute hyperbaric exposure in the rat. Undersea & hyperbaric medicine : journal of the Undersea and Hyperbaric Medical Society, Inc. 1998;25(4):217-21. Epub 1999/01/12.
27. Ward CA, McCullough D, Yee D, Stanga D, Fraser WD. Complement activation involvement in decompression sickness of rabbits. Undersea biomedical research. 1990;17(1):51-66. Epub 1990/01/01.
28. Sykes JJ, Yaffe LJ. Light and electron microscopic alterations in spinal cord myelin sheaths after decompression sickness. Undersea biomedical research. 1985;12(3):251-8. Epub 1985/09/01.
29. Francis TJ, Pezeshkpour GH, Dutka AJ, Hallenbeck JM, Flynn ET. Is there a role for the autochthonous bubble in the pathogenesis of spinal cord decompression sickness? Journal of neuropathology and experimental neurology. 1988;47(4):475-87. Epub 1988/07/01.
30. Hills BA, James PB. Spinal decompression sickness: mechanical studies and a model. Undersea biomedical research. 1982;9(3):185-201. Epub 1982/09/01.
31. Van Liew HD, Burkard ME. Simulation of gas bubbles in hypobaric decompressions: roles of O₂, CO₂, and H₂O. Aviat Space Environ Med. 1995;66(1):50-5. Epub 1995/01/01.
32. Foster PP, Feiveson AH, Glowinski R, Izygon M, Boriek AM. A model for influence of exercise on formation and growth of tissue bubbles during altitude decompression. Am J Physiol Regul Integr Comp Physiol. 2000;279(6):R2304-16. Epub 2000/11/18.
33. Hills BA. Decompression sickness. New York: John Wiley & Sons. 1977;vol. 1.:239.
34. Van Liew HD, Conkin J, Burkard ME. The oxygen window and decompression bubbles: estimates and significance. Aviation, space, and environmental medicine. 1993;64(9 Pt 1):859-65. Epub 1993/09/01.
35. Van Liew HD, Bishop B, Walder P, Rahn H. Effects of compression on composition and absorption of tissue gas pockets. J Appl Physiol. 1965;20(5):927-33. Epub 1965/09/01.
36. Foster PP, Conkin J, Powell MR, Waligora JM, Chhikara RS. Role of metabolic gases in bubble formation during hypobaric exposures. J Appl Physiol. 1998;84(3):1088-95. Epub 1998/04/16.
37. Burkard ME, Van Liew HD. Simulation of exchanges of multiple gases in bubbles in the body. Respir Physiol. 1994;95(2):131-45. Epub 1994/02/01.
38. Hyldegaard O, Madsen J. Effect of hypobaric air, oxygen, heliox (50:50), or heliox (80:20) breathing on air bubbles in adipose tissue. J Appl Physiol. 2007;103(3):757-62. Epub 2007/06/30.
39. Randsoe T, Kvist TM, Hyldegaard O. Effect of oxygen and heliox breathing on air bubbles in adipose tissue during 25-kPa altitude exposures. J Appl Physiol. 2008;105(5):1492-7. Epub 2008/08/30.
40. Lowe KC. Perfluorocarbons as oxygen-transport fluids. Comparative biochemistry and physiology A, Comparative physiology. 1987;87(4):825-38. Epub 1987/01/01.
41. Spiess BD. Perfluorocarbon emulsions as a promising technology: a review of tissue and vascular gas dynamics. J Appl Physiol. 2009;106(4):1444-52. Epub 2009/01/31.
42. Spiess BD. Perfluorocarbon emulsions: one approach to intravenous artificial respiratory gas transport. International anesthesiology clinics. 1995;33(1):103-13. Epub 1995/01/01.
43. Clark LC, Jr., Gollan F. Survival of mammals breathing organic liquids equilibrated with oxygen at atmospheric pressure. Science. 1966;152(3730):1755-6. Epub 1966/06/24.
44. Henkel-Honke T, Oleck M. Artificial oxygen carriers: a current review. AANA journal. 2007;75(3):205-11. Epub 2007/06/27.
45. Spiess BD, McCarthy RJ, Tuman KJ, Woronowicz AW, Tool KA, Ivankovich AD. Treatment of decompression sickness with a perfluorocarbon emulsion (FC-43). Undersea biomedical research. 1988;15(1):31-7. Epub 1988/01/01.
46. Lutz J, Herrmann G. Perfluorochemicals as a treatment of decompression sickness in rats. Pflugers Archiv : European journal of physiology. 1984;401(2):174-7. Epub 1984/06/01.

47. Lynch PR, Krasner LJ, Vinciguerra T, Shaffer TH. Effects of intravenous perfluorocarbon and oxygen breathing on acute decompression sickness in the hamster. *Undersea biomedical research*. 1989;16(4):275-81. Epub 1989/07/01.
48. Dainer H NJ, Brass K, Montcalm-Smith E, Mahon R. Short oxygen prebreathing and intravenous perfluorocarbon emulsion reduces morbidity and mortality in a swine saturation model of decompression sickness. *J Appl Physiol*. 2007;102:1099-104.
49. Dromsky DM SB, Fahlman A. Treatment of decompression sickness in swine with intravenous perfluorocarbon emulsion. *Aviat Space Environ Med*. 2004;75:301-5.
50. Zhu J, Hullett JB, Somera L, Barbee RW, Ward KR, Berger BE, et al. Intravenous perfluorocarbon emulsion increases nitrogen washout after venous gas emboli in rabbits. *Undersea & hyperbaric medicine : journal of the Undersea and Hyperbaric Medical Society, Inc*. 2007;34(1):7-20. Epub 2007/03/31.
51. Torres Filho IP, Torres LN, Spiess BD. In vivo microvascular mosaics show air embolism reduction after perfluorocarbon emulsion treatment. *Microvascular research*. 2012;84(3):390-4. Epub 2012/09/27.
52. Cochran RP, Kunzelman KS, Vocelka CR, Akimoto H, Thomas R, Soltow LO, et al. Perfluorocarbon emulsion in the cardiopulmonary bypass prime reduces neurologic injury. *The Annals of thoracic surgery*. 1997;63(5):1326-32. Epub 1997/05/01.
53. Lundgren C, Bergoe G, Olszowka A, Tyssebotn I. Tissue nitrogen elimination in oxygen-breathing pigs is enhanced by fluorocarbon-derived intravascular micro-bubbles. *Undersea & hyperbaric medicine : journal of the Undersea and Hyperbaric Medical Society, Inc*. 2005;32(4):215-26. Epub 2005/10/22.
54. Spiess BD, McCarthy R, Piotrowski D, Ivankovich AD. Protection from venous air embolism with fluorocarbon emulsion FC-43. *The Journal of surgical research*. 1986;41(4):439-44. Epub 1986/10/01.
55. Spiess BD, McCarthy RJ, Tuman KJ, Ivankovich AD. Protection from coronary air embolism by a perfluorocarbon emulsion (FC-43). *Journal of cardiothoracic anesthesia*. 1987;1(3):210-5. Epub 1987/06/01.
56. Eckmann DM, Lomivorotov VN. Microvascular gas embolization clearance following perfluorocarbon administration. *J Appl Physiol*. 2003;94(3):860-8. Epub 2003/02/07.
57. Herren JI, Kunzelman KS, Vocelka C, Cochran RP, Spiess BD. Horseradish peroxidase as a histological indicator of mechanisms of porcine retinal vascular damage and protection with perfluorocarbons after massive air embolism. *Stroke; a journal of cerebral circulation*. 1997;28(10):2025-30. Epub 1997/10/28.
58. Herren JI, Kunzelman KS, Vocelka C, Cochran RP, Spiess BD. Angiographic and histological evaluation of porcine retinal vascular damage and protection with perfluorocarbons after massive air embolism. *Stroke; a journal of cerebral circulation*. 1998;29(11):2396-403. Epub 1998/11/06.
59. Yoshitani K, de Lange F, Ma Q, Grocott HP, Mackensen GB. Reduction in air bubble size using perfluorocarbons during cardiopulmonary bypass in the rat. *Anesthesia and analgesia*. 2006;103(5):1089-93. Epub 2006/10/24.
60. Novotny JA BB, Himm JF, Homer LD. Quantifying the effect of intravascular perfluorocarbon on xenon elimination from canine muscle. *J Appl Physiol*. 1993;74:1356-60.
61. Eckmann DM, Armstead SC. Influence of endothelial glycocalyx degradation and surfactants on air embolism adhesion. *Anesthesiology*. 2006;105(6):1220-7. Epub 2006/11/24.
62. Riess JG. Perfluorocarbon-based oxygen delivery. *Artificial cells, blood substitutes, and immobilization biotechnology*. 2006;34(6):567-80. Epub 2006/11/09.
63. Spahn DR. Blood substitutes. *Artificial oxygen carriers: perfluorocarbon emulsions*. *Crit Care*. 1999;3(5):R93-7. Epub 2000/11/30.
64. Spahn DR, Kocian R. Artificial O₂ carriers: status in 2005. *Current pharmaceutical design*. 2005;11(31):4099-114. Epub 2005/12/28.
65. Riess JG. Understanding the fundamentals of perfluorocarbons and perfluorocarbon emulsions relevant to in vivo oxygen delivery. *Artificial cells, blood substitutes, and immobilization biotechnology*. 2005;33(1):47-63. Epub 2005/03/17.
66. Mollerlokken A, Berge VJ, Jorgensen A, Wisloff U, Brubakk AO. Effect of a short-acting NO donor on bubble formation from a saturation dive in pigs. *J Appl Physiol*. 2006;101(6):1541-5. Epub 2006/07/22.
67. Dujic Z, Palada I, Valic Z, Duplancic D, Obad A, Wisloff U, et al. Exogenous nitric oxide and bubble formation in divers. *Medicine and science in sports and exercise*. 2006;38(8):1432-5. Epub 2006/08/05.
68. Wisloff U, Richardson RS, Brubakk AO. Exercise and nitric oxide prevent bubble formation: a novel approach to the prevention of decompression sickness? *The Journal of physiology*. 2004;555(Pt 3):825-9. Epub 2004/01/16.
69. Wisloff U, Richardson RS, Brubakk AO. NOS inhibition increases bubble formation and reduces survival in sedentary but not exercised rats. *The Journal of physiology*. 2003;546(Pt 2):577-82. Epub 2003/01/16.
70. Bondi M, Cavaggioni A, Michieli P, Schiavon M, Travain G. Delayed effect of nitric oxide synthase inhibition on the survival of rats after acute decompression. *Undersea & hyperbaric medicine : journal of the Undersea and Hyperbaric Medical Society, Inc*. 2005;32(2):121-8. Epub 2005/06/02.
71. Moon RE. Nitroglycerine: relief from the heartache of decompression sickness? *J Appl Physiol*. 2006;101(6):1537-8. Epub 2006/07/15.
72. Hyldegaard O, Jensen T. Effect of heliox, oxygen and air breathing on helium bubbles after heliox diving. *Undersea & hyperbaric medicine : journal of the Undersea and Hyperbaric Medical Society, Inc*. 2007;34(2):107-22. Epub 2007/05/25.
73. Hyldegaard O, Kerem D, Melamed Y. Effect of combined recompression and air, oxygen, or heliox breathing on air bubbles in rat tissues. *J Appl Physiol*. 2001;90(5):1639-47. Epub 2001/04/12.
74. Hyldegaard O, Kerem D, Melamed Y. Effect of isobaric breathing gas shifts from air to heliox mixtures on resolution of air bubbles in lipid and aqueous tissues of recompressed rats. *European journal of applied physiology*. 2011;111(9):2183-93. Epub 2011/02/15.
75. Hyldegaard O, Madsen J. Effect of air, heliox, and oxygen breathing on air bubbles in aqueous tissues in the rat. *Undersea & hyperbaric medicine : journal of the Undersea and Hyperbaric Medical Society, Inc*. 1994;21(4):413-24. Epub 1994/12/01.
76. Hyldegaard O, Madsen J. Effect of SF₆-O₂ (80/20) breathing on air bubbles in rat tissues. *Undersea & hyperbaric medicine : journal of the Undersea and Hyperbaric Medical Society, Inc*. 1995;22(4):355-65. Epub 1995/12/01.
77. Hyldegaard O, Moller M, Madsen J. Effect of He-O₂, O₂, and N₂O-O₂ breathing on injected bubbles in spinal white matter. *Undersea biomedical research*. 1991;18(5-6):361-71. Epub 1991/09/01.

78. Hyldegaard O, Moller M, Madsen J. Protective effect of oxygen and heliox breathing during development of spinal decompression sickness. *Undersea & hyperbaric medicine : journal of the Undersea and Hyperbaric Medical Society, Inc.* 1994;21(2):115-28. Epub 1994/06/01.
79. Hyldegaard O, Madsen J. Influence of heliox, oxygen, and N2O-O2 breathing on N2 bubbles in adipose tissue. *Undersea biomedical research.* 1989;16(3):185-93. Epub 1989/05/01.
80. Abrams J. Hemodynamic effects of nitroglycerin and long-acting nitrates. *American heart journal.* 1985;110(1 Pt 2):216-24. Epub 1985/07/01.
81. Markos F, Ruane O'Hora T, Noble MI. What is the mechanism of flow-mediated arterial dilatation. *Clinical and experimental pharmacology & physiology.* 2013;40(8):489-94. Epub 2013/05/23.
82. Loos D, Schneider R, Schorner W. Changes in regional body blood volume caused by nitroglycerin. *Zeitschrift fur Kardiologie.* 1983;72 Suppl 3:29-32. Epub 1983/01/01.
83. Mason DT, Braunwald E. The effects of nitroglycerin and amyl nitrite on arteriolar and venous tone in the human forearm. *Circulation.* 1965;32(5):755-66. Epub 1965/11/01.
84. Leier CB, Magorien RD, Desch CE, Thompson MJ, Unverferth DV. Hydralazine and isosorbide dinitrate: comparative central and regional hemodynamic effects when administered alone or in combination. *Circulation.* 1981;63(1):102-9. Epub 1981/01/01.
85. Tzeng TB, Fung HL. Pharmacokinetic/pharmacodynamic relationship of the duration of vasodilating action of organic mononitrates in rats. *The Journal of pharmacology and experimental therapeutics.* 1992;261(2):692-700. Epub 1992/05/01.
86. Rasband W. Image. *Image Processing and Analysis (version 1.61).* Washington DCS: National Institutes of Health Research Services Branch, NIMH USA. <http://rsb.info.nih.gov/nih-image/download.html>. 1996.
87. Manabe T, Yamamoto A, Satoh K, Ichihara K. Tolerance to nitroglycerin induced by isosorbide-5-mononitrate infusion in vivo. *Biological & pharmaceutical bulletin.* 2001;24(12):1370-2. Epub 2002/01/05.
88. Hedenqvist P, Hellebrekers LJ. Laboratory animal analgesia, anesthesia, and euthanasia. In: Hau J, Hoosier GL Jr, editors. *Handbook of laboratory animal science.* Boca Raton: CRC Press LLC; 2003. pp. 413-455.
89. Roughan JV, Ojeda OB, Flecknell PA. The influence of pre-anaesthetic administration of buprenorphine on the anaesthetic effects of ketamine/medetomidine and pentobarbitone in rats and the consequences of repeated anaesthesia. *Laboratory animals.* 1999;33(3):234-42. Epub 2000/04/26.
90. Torbati D, Ramirez J, Hon E, Camacho MT, Sussman JB, Raszynski A, et al. Experimental critical care in rats: gender differences in anesthesia, ventilation, and gas exchange. *Critical care medicine.* 1999;27(9):1878-84. Epub 1999/10/03.
91. Zambricki EA, Dalecy LG. Rat sex differences in anesthesia. *Comparative medicine.* 2004;54(1):49-53. Epub 2004/03/19.
92. Castillo C, Asbun J, Escalante B, Villalon CM, Lopez P, Castillo EF. Thiopental inhibits nitric oxide production in rat aorta. *Canadian journal of physiology and pharmacology.* 1999;77(12):958-66. Epub 1999/12/22.
93. Kessler P, Kronemann N, Hecker M, Busse R, Schini-Kerth VB. Effects of barbiturates on the expression of the inducible nitric oxide synthase in vascular smooth muscle. *Journal of cardiovascular pharmacology.* 1997;30(6):802-10. Epub 1998/01/22.
94. Kim SO, Toda H, Nakamura K, Miyawaki I, Hirakata H, Hirata S, et al. Thiopental attenuates relaxation and cyclic GMP production in vascular smooth muscle of endotoxin-treated rat aorta, independent of nitric oxide production. *British journal of anaesthesia.* 1998;81(4):601-2. Epub 1999/01/30.
95. GraphPad. *Instat version 3.06 for windows.* San Diego, CA, USA. 2003.
96. SPSS. *Statistical Package of the Social Sciences.* Chicago, IL: SPSS, 1998.
97. Randsoe T, Meehan CF, Broholm H, Hyldegaard O. Effect of nitric oxide on spinal evoked potentials and survival rate in rats with decompression sickness. *J Appl Physiol (1985).* 2015;118(1):20-8. Epub 2014/11/08.
98. Van Liew HD, Hlastala MP. Influence of bubble size and blood perfusion on absorption of gas bubbles in tissues. *Respir Physiol.* 1969;7(1):111-21. Epub 1969/06/01.
99. Hyldegaard O. *Treatment of Decompression Sickness During Breathing of Oxygen and Inert Gases.* Doctoral Thesis, University of Copenhagen, Sept 7.th, 2012. Pp 1-106, ISBN 978-87-995449-0-5.
100. Madsen J, Malchow-Moller A, Waldorff S. Continuous estimation of adipose tissue blood flow in rats by 133Xe elimination. *J Appl Physiol.* 1975;39(5):851-6. Epub 1975/11/01.
101. WF G. Pulmonary function. In: *Review of Medical Physiology:* Los Altos: Lange Medical Publications; 1983.
102. Behnke AR. The isobaric (oxygen window) principle of decompression. *The New Thrust Seaward Trans 3rd Annual Conf Marine Tech Soc; San Diego Washington DC: Marine Technology Society; 1967.*
103. Randsoe T, Hyldegaard O. Effect of oxygen breathing on micro oxygen bubbles in nitrogen-depleted rat adipose tissue at sea level and 25 kPa altitude exposures. *J Appl Physiol.* 2012;113(3):426-33. Epub 2012/06/02.
104. Webb JT, Pilmanis AA, O'Connor RB. An abrupt zero-preoxygenation altitude threshold for decompression sickness symptoms. *Aviation, space, and environmental medicine.* 1998;69(4):335-40. Epub 1998/04/30.
105. Flaim SF. Pharmacokinetics and side effects of perfluorocarbon-based blood substitutes. *Artificial cells, blood substitutes, and immobilization biotechnology.* 1994;22(4):1043-54. Epub 1994/01/01.
106. Randsoe T, Hyldegaard O. Effect of oxygen breathing and perfluorocarbon emulsion treatment on air bubbles in adipose tissue during decompression sickness. *J Appl Physiol.* 2009;107(6):1857-63. Epub 2009/10/24.
107. Brod VI K, Hirsh M, Adir Y, Bittermann H. Hemodynamic effects of combined treatment with oxygen and hypertonic saline in hemorrhagic shock. *Critical care medicine.* 2006;34:2784-91.
108. Sakai H M, Horinouchi H, Yamamoto M, Ikeda E, Takeoka S, Kobayashi K. Hemoglobin-vesicles suspended in recombinant human serum albumin for resuscitation from hemorrhagic shock in anesthetized rats. *Critical care medicine.* 2004;32:539-45.
109. Butler GJ, Al-Waili N, Passano DV, Ramos J, Chavarri J, Beale J, et al. Altitude mountain sickness among tourist populations: a review and pathophysiology supporting management with hyperbaric oxygen. *Journal of medical engineering & technology.* 2011;35(3-4):197-207. Epub 2010/09/15.
110. Willie CK, Smith KJ, Day TA, Ray LA, Lewis NC, Bakker A, et al. Regional cerebral blood flow in humans at high altitude: Gradual ascent and two weeks at 5050m. *J Appl Physiol.* 2013. Epub 2013/07/03.

111. Yount D, Strauss R. On the evolution, generation and regeneration of gas cavitation nuclei. *J Acoust Soc AM* 65: 1431–1439, 1982.
112. Kirsten R, Nelson K, Kirsten D, Heintz B. Clinical pharmacokinetics of vasodilators. Part II. Clinical pharmacokinetics. 1998;35(1):9-36. Epub 1998/07/23.
113. Abrams J. Nitroglycerin and long-acting nitrates. *The New England journal of medicine*. 1980;302(22):1234-7. Epub 1980/05/29.
114. Jersey SL, Baril RT, McCarty RD, Millhouse CM. Severe neurological decompression sickness in a U-2 pilot. *Aviat Space Environ Med*. 2010;81(1):64-8. Epub 2010/01/12.
115. Bendrick GA, Ainscough MJ, Pilmanis AA, Bisson RU. Prevalence of decompression sickness among U-2 pilots. *Aviation, space, and environmental medicine*. 1996;67(3):199-206. Epub 1996/03/01.
116. Pickard BJ. Altitude decompression sickness in a pilot wearing a pressure suit above 70,000 feet. *Aviation, space, and environmental medicine*. 2003;74(4):357-9. Epub 2003/04/12.
117. Nunn JF. Respiratory aspects of high altitude and space, In: *Applied Respiratory Physiology*. Oxford, UK: Butterworth-Heinemann; 1994, vol. 1, p. 338–352.
118. Muehlberger PM, Pilmanis AA, Webb JT, Olson JE. Altitude decompression sickness symptom resolution during descent to ground level. *Aviat Space Environ Med*. 2004;75(6):496-9. Epub 2004/06/17.
119. Dart TS, Butler W. Towards new paradigms for the treatment of hypobaric decompression sickness. *Aviat Space Environ Med*. 1998;69(4):403-9. Epub 1998/04/30.
120. Zamboni WA, Allan CR., Robert CR., Graham H., Suchy H., O. Kuchan J. Morphologic Analysis of the Microcirculation During Reperfusion of Ischemic Skeletal Muscle and the Effect of Hyperbaric Oxygen. *Plastic and Reconstructive Surgery*. 1993;91, No.6:1110-23.
121. Bergø G.W. TI. Effect of exposure to oxygen at 101 and 150 kPa on the cerebral circulation and oxygen supply in conscious rats. *Eur J Appl Physiol*. 1995;71(6):475-84.
122. Bergø G.W., Tyssebotn I. Cerebral blood flow distribution during exposure to 5 bar oxygen in awake rats. *Undersea Biomedical Research*. 1992;19:339-54.
123. Clark J.M. Oxygen Toxicity. In *The Physiology and Medicine of Diving*. 1993:121-70. Epub Fourth edition.
124. Mahon RT DH, Nelson JW. . Decompression sickness in a swine model: isobaric denitrogenation and perfluorocarbon at depth. *Aviat Space Environ Med*. 2006;77:8-12.
125. Shu J H, Somera L, Barbee RW, Ward KR, Berger BE, Spiess BD. Intravenous perfluorocarbon emulsion increases nitrogen washout after venous gas emboli in rabbits. *Undersea Hyperb Med*. 2007;34:7-20.
126. Mahon RT, Hall A, Bodo M, Auken C. The intravenous perfluorocarbon emulsion Oxycyte does not increase hyperbaric oxygen-related seizures in a non-sedated swine model. *European journal of applied physiology*. 2013;113(11):2795-802. Epub 2013/09/26.
127. US-Navy. *US Navy Diving Manual 2001*. Washington DC: Naval Sea Systems Command; 1999.
128. C. W. Complement activation involvement in decompression sickness of rabbits. *Undersea Biomed Res*. 1990;17:51-66.
129. Moon RE. G, DF. Treatment of the Decompression Disorders. In: Brubakk AO NT, editor. *Physiology and Medicine of Diving*. 5th ed. Cornwall: Saunders; 2003. p. 600-50.
130. Tetzlaff K SE, Muth CM. Evaluation and management of decompression illness---an intensivist's perspective. *Intensive Care Med*. 2003;29:2128-36.
131. Moncada S, Palmer RM, Higgs EA. Nitric oxide: physiology, pathophysiology, and pharmacology. *Pharmacological reviews*. 1991;43(2):109-42. Epub 1991/06/01.
132. Bult H. Nitric oxide and atherosclerosis: possible implications for therapy. *Molecular medicine today*. 1996;2(12):510-8. Epub 1996/12/01.
133. Sanders DB, Kelley T, Larson D. The role of nitric oxide synthase/nitric oxide in vascular smooth muscle control. *Perfusion*. 2000;15(2):97-104. Epub 2000/05/02.
134. Stamler JS, Meissner G. Physiology of nitric oxide in skeletal muscle. *Physiological reviews*. 2001;81(1):209-37. Epub 2001/01/12.
135. Waligora JM, Horrigan DJ, Jr., Conkin J. The effect of extended O2 prebreathing on altitude decompression sickness and venous gas bubbles. *Aviat Space Environ Med*. 1987;58(9 Pt 2):A110-2. Epub 1987/09/01.
136. Webb JT, Pilmanis AA. Preoxygenation time versus decompression sickness incidence. *Safe journal*. 1999;29(2):75-8. Epub 2002/01/05.
137. Randsoe T, Hyldegaard O. Threshold altitude for bubble decay and stabilization in rat adipose tissue at hypobaric exposures. *Aviation, space, and environmental medicine*. 2013;84(7):675-83. Epub 2013/07/17.
138. Randsoe T, Hyldegaard O. Treatment of micro air bubbles in rat adipose tissue at 25 kPa altitude exposures with perfluorocarbon emulsions and nitric oxide. *European journal of applied physiology*. 2013. Epub 2013/10/26.